Response to Referees

We thank both referees for their comments and suggestions. The manuscript was revised to thoroughly address each point. Generally the plan was executed as follows:

(1) The description of the simulations analyzed in our study was improved by adding more details concerning (a) how the different simulations (ORCA2, ORCA05, and ORCA025) were made, making it clear that each of these has its own control simulation, (b) how CFC-12 was simulated, and (c) how carbon transport was estimated at the boundaries of the Arctic Ocean.

(2) The discussion section was expanded to provide more detail about (a) the effect of increasing resolution in ocean models found by other modeling studies and (b) the mechanisms influencing changes in air-sea CO_2 fluxes in the Arctic between the different resolutions. Additional analysis were also included to show how the different configurations compare to each other in terms of the global-ocean inventory of anthropogenic carbon.

During the review period, we also discovered an issue with our CFC-12 simulations (initialization to non-zero concentrations). Hence we have rerun all CFC-12 simulations (following details in the revised manuscript). Furthermore, we have used the opportunity to complement the ORCA05 C_{ant} perturbation simulations with analogous simulations for the ORCA2 and ORCA025 configurations (each initialized in the beginning of 1958 with output from the last time step in 1957 of the ORCA05 C_{ant} perturbation simulation and run until 2012). With these updated simulations, the model-data CFC-12 comparison has been improved (as discussed in Sections 3.2 and 4.1) along with the corrections for the estimated C_{ant} fluxes at the boundaries (both lateral and at the air-sea interface). The figures and tables of the revised manuscript are updated accordingly. Despite these improvements, the Conclusions of our study remain the same.

In the following we address the concerns of the Reviewers point by point.

Referee # 1

1) Overview

Terhaar et al. ask: what effect does model resolution have on simulated Arctic Ocean anthropogenic CO_2 storage and acidification? The answer: increased model resolution shows higher regional storage by up to 25%, moving the inventory closer to data-based estimates, and increased acidification with faster shoaling of the aragonite saturation horizon. This is an interesting and useful question, and the study has been well-designed to answer it. The results and their interpretation seem sensible, although as mentioned below, a robust uncertainty analysis is critically lacking. The manuscript is interesting and easy to read. The Introduction is very well-written and Methods are clear. Results and Discussion are succinct, but in places the Discussion in particular could be developed further to provide more insight. Many of the questions below are really prompts in this direction.

Reply: Thank you very much. In the revised manuscript, we have strived to address these concerns in detail.

2) Scientific questions

Reviewer Question 1 — The highest-resolution model is "still not eddy resolving" (3-28 i.e. page 3, line 28). Does that mean that you would expect further changes still with yet higher resolution? Would you expect the anthropogenic CO_2 inventory to increase even more?

Reply: Without actually making higher resolution simulations, one can of course never be certain. However, we would agree with Referee #1 that the anthropogenic carbon inventory in the Arctic Ocean would probably increase if the model resolution was refined even further. The C_{ant} inventory in 2005 increases by 0.38 Pg C between ORCA2 and ORCA05 and by 0.27 Pg C between ORCA05 and ORCA025, so we may not have reached the nearly flat part of the asymptote. Further enhancement of resolution could further increase the inventory via the combined effects of improved bathymetry, increased coastal water velocities, and enhanced surface-to-deep transport of passive tracers from brine formation on Arctic shelves. Concerning the latter, even higher model resolution might well lead to higher C_{ant} concentrations in the Canada basin and to refining the chimneys of higher CFC-12 concentrations in the Canada basin, which are observed but only barely resolved in ORCA025 (page 10, lines 23-24). We propose the following change in section 4.4 of the revised manuscript:

Proposed change: A signature of this source in the observed sections may be the chimneys of constant CFC-12 concentration from the surface to about 1000 m in the Canada basin, features for which only ORCA025 exhibits any such signature, albeit faint. To adequately model lateral ~~fluxes of C_{ant}~~ exchanges of C_{ant} in the Arctic Ocean, at least a resolution comparable to that used in ORCA05 may be needed, while resolutions comparable to that in ORCA025 or above may well be required to begin to capture the effects from density flows along the slope. As a consequence of the deficient representation of these density flows, we would expect to see an increase in C_{ant} when using even higher resolution. (page 16, lines 11–16 in the revised manuscript)

Reviewer Question 2 — The monthly averaging process introduces an error of 27% for the lowest-resolution model (7-20). This is a similar magnitude to the difference in anthropogenic CO_2 inventory between the different resolutions, which is your most important result. Does this error being the same size as the 'signal' not significantly reduce your confidence in the results (i.e. differences between resolutions)?

Reply: Our error estimate of 27% applies only to the ORCA2 transport of C_{ant} calculated separately at each of the 4 boundaries of the Arctic Ocean from monthly-average model output (offline), an important point raised by Referee #1 for which we should have been clearer. That offline calculation error is smaller at higher resolution (e.g, 4% with ORCA025). Moreover, it does not apply to our estimates of C_{ant} inventory, the cumulative air-sea C_{ant} flux, and the total lateral flux, all of which are calculated online in the model and for which associated calculation errors are negligible.

Proposed change: The relative error for transport of C_{ant} across the separate boundaries introduced by the monthly average calculations is ~~27~~28% for ORCA2, 7% for ORCA05, and ~~4~~3% for ORCA025. Note that this error applies neither to the C_{ant} inventory, nor to the cumulative air-sea flux or the lateral fluxes, which are all calculated 'online', during the simulations. (page 8, lines 9–11 in the revised manuscript)

Reviewer Question 3 — You note that overestimation of sea-ice cover should reduce air-sea CO_2 exchange (9-14). There are a number of observational studies that attempt to quantify this effect. Can these be used to quantify your statement?

Reply: Our overestimation of sea-ice extent is less than 3%. Thus it is of second order when estimating the C_{ant} air-sea flux. There are studies that have estimated the effect of declining sea-ice on air-sea fluxes of total carbon (Bates et al. [2006], Cai et al. [2010]), but they do not agree on whether the flux will increase due to increasing biological activity or decrease due to higher stratification and increases in riverine organic carbon. Because these studies focus on the air-sea flux of total CO_2 (natural + anthropogenic), we cannot use them to extract the response of only the anthropogenic component, the focus of our study.

Reviewer Question 4 — Section 3.4: my impression was that the primary reason to expect model resolution to influence the anthropogenic CO_2 inventory was because of better representation of circulation features. Therefore the increase in lateral flux, being a function of circulation, is expected – but the simultaneous increase in the air-sea flux does not seem so intuitive. Indeed if additional anthropogenic CO_2 is being transported into the region from elsewhere we might expect this to increase total dissolved inorganic carbon and thus reduce net air-to-sea CO_2 flux. Do you have a conceptual explanation for what is driving the air-sea flux increase with resolution?

Reply: Two mechanisms may explain the increase in the air-sea flux with resolution: (1) higher resolution increases the amount of C_{ant} that is advected into the Arctic Ocean through the Fram Strait via subsurface currents, which does not substantially affect surface C_{ant} concentrations nor hence air-sea exchange of anthropogenic carbon and (2) higher resolution enhances deep-water formation in the Arctic Ocean, mainly in the Barents Sea as shown in the CFC-12 profiles (Figure 7), which reduces surface C_{ant} and thus enhances the air-to-sea flux of anthropogenic carbon.

Proposed change: With increasing water inflow, the inflow of C_{ant} is also increased. Although more C_{ant} is entering the Arctic Ocean, the air-sea C_{ant} flux into the Arctic Ocean increases with resolution. This apparent contradiction can be explained by two mechanism: (1) Higher resolution increases the inflow of C_{ant} through the Fram Strait, which is mainly occurring in subsurface currents and therefore does not substantially impact surface C_{ant} concentrations nor hence air-sea exchanges of C_{ant} and (2) higher resolution enhances deep-water formation, mainly in the Barents Sea, which reduces surface C_{ant} and thus enhances the air-to-sea flux of C_{ant}. Although the air-sea flux increases slightly, the larger lateral water fluxes in ORCA05 and ORCA025 ~~largely~~ mainly explain their higher ~~C_{ant}~~ C_{ant} concentrations in the Nansen and Amundsen basins. (page 15, lines 27–34 in the revised manuscript)

Reviewer Question 5 — In order to declare that two things are 'not statistically different' (14-12) you must also provide the statistical information that were used to demonstrate this.

Reply: In the revised manuscript, the corresponding sentence is changed to 'The simulated air-sea flux falls within that assigned uncertainty range for the data-based estimate.'

Proposed change: ~~Given that large uncertainty , the modeled and data-based estimates of the~~ The simulated air-sea ~~flux are not statistically different~~flux falls within that assigned uncertainty range for the data-based estimate. (page 15, lines 18–19 in the revised manuscript)

Reviewer Question 6 — Does the increase in resolution alter lateral anthropogenic CO_2 fluxes primarily because of the representation of circulation (1) inside the Arctic Ocean, (2) at its boundaries/interfaces, (3) in the non-Arctic global ocean, or (4) everywhere?

Reply: We tried to address this question in Section 4.4 of the submitted manuscript, but we only discuss circulation differences inside the Arctic Ocean and at its boundaries. We showed that increasing resolution from ORCA2 to ORCA05 affects mainly the circulation at the boundaries (1) while the change from ORCA05 to ORCA025 affects mainly circulation inside the Arctic Ocean (2).

For more insight into the role of the global ocean (outside the Arctic), we have now calculated the total C_{ant} inventory for the global ocean with all three resolutions (see below). Globally the three resolutions agree within 3%. This agreement is much tighter than that for the Arctic Ocean C_{ant} inventory. This new comparison suggests a weak role of the non-Arctic global ocean on the Arctic Ocean C_{ant} budget (3)(4), although resolution-dependent changes in regions adjacent to the Arctic Ocean's lateral boundaries (e.g., in the North Atlantic) may well have an effect. These considerations are added to section 4.4 of the revised manuscript.

Proposed change: The change from ORCA2 to ORCA05 seems to mainly improve lateral exchanges with adjacent oceans, while the change from ORCA05 to ORCA025 improves inner-Arctic Ocean circulation. (page 16, lines 4–6 in the revised manuscript)

Reviewer Question 7 — You note that for computational reasons we cannot routinely run these models globally at high resolution, but if only one region of the model needed to be at high resolution to achieve your results, would it be possible to strike a balance with a hybrid resolution model?

Reply: Certainly such approaches, using for example the nesting tool of NEMO (AGRIF, Debreu et al. [2008]) as in Duteil et al. [2014] would be an interesting option. Unfortunately, this nesting tool is known to not work well in ice-covered regions nor with the biogeochemical model PISCES. Hence we leave this for future work as is mentioned in the Conclusion of the revised manuscript.

Proposed change: For such regional studies, nested models would offer the advantage of focused higher resolution while still avoiding adverse effects from imposed lateral boundary conditions. (page 18, lines 31–32 in the revised manuscript)

Reviewer Question 8 — Some of the notes about possible future work on CFC-12 and the TTD parameters in the Conclusions would probably be more suited to the Discussion.

Reply: We considered moving these notes to the Discussion, but decided against it as it is rather an outlook than a discussion of results.

Reviewer Question 9 — No other studies have been mentioned that have attempted to answer this same question for the Arctic Ocean, but there have been other investigations of the effect of increased model resolution in various contexts. Do these provide any insights that would be useful in interpreting your results?

Reply: In terms of ocean biogeochemistry, most studies on the effect of resolution have focused on the impacts of mesoscale to submesoscale structures on phytoplankton and productivity (e.g., Lévy [2008],

McGillicuddy [2016]). Other studies have investigated the role of increased model resolution on transient tracers (Lachkar et al., [2007]) and on carbon and oxygen (Duteil et al., [2014]), but they have focused on other regions (Southern Ocean and the tropics). Therefore it is difficult to transfer their findings to the Arctic Ocean. Some mention on other studies focusing on the role of model resolution is included in the Discussion of the revised manuscript.

Proposed change:
Similar to our results in the Arctic Ocean, improving circulation with higher model resolution has also been shown to be the key driver for an improved representation of anthropogenic tracers in the Southern Ocean (Lachkar et al., 2007) or oxygen concentrations in the tropics (Duteil et al., 2014).(page 16, lines 17–19)

3) Figures

Reviewer Question 10 — Use of red vs green (e.g. Fig. 3) with no difference in line style can render these lines indistinguishable to colorblind readers.

Reviewer Question 11 — The blue-green-yellow-red color scale used on transect plots (e.g. Fig. 4) is not perceptually uniform, leading to visual artifacts such as false boundaries.

Reviewer Question 12 — Depth should be positive going down into the ocean (Figs. 4 and 6).

Reply: These suggestions for improving the style and colors will be implemented in the revised manuscript.

4) Technical/grammatical notes

Reviewer Question 13 — There is inconsistency in usage of past and present tenses in the Methods.

Reply: The Methods section will be improved to avoid this inconsistency in the revised manuscript.

Reviewer Question 14 — The contexts in which the word 'though' is used are highly colloquial and, to me, not suited for scientific writing (2-12, 14-29, 15-8).

Reply: We avoid the use of the word 'though' in the revised manuscript.

Reviewer Question 15 — Suggested corrections:
1-6 eddy-admitting
2-3 consequences for
4-30 following Moore et al.
10-24 (Fig. 6) ?
11-21 Arctic Ocean basins
15-33 reword this sentence to indicate the direction of the effect

Reply: The manuscript will be revised according to these suggestions. For 15-33 we will write "Thus model resolution also affects the time at which waters become undersaturated with respect to aragonite with higher resolutoin producing greater shoaling."

References

Bates, N. and Mathis, J. (2009). The Arctic Ocean marine carbon cycle: evaluation of air-sea CO2 exchanges, ocean acidification impacts and potential feedbacks. Biogeosciences, 6(11):2433–2459. 8

Cai, W.-J., Chen, L., Chen, B., Gao, Z., Lee, S. H., Chen, J., Pierrot, D., Sullivan, K., Wang, Y., Hu, X., et al. (2010). Decrease in the CO2 uptake capacity in an ice-free arctic ocean basin. Science, 329(5991):556–559. 2

Debreu, L., Vouland, C. and Blayo, E. AGRIF: Adaptive grid refinement in Fortran. Computers Geosci. 34, 8–13 (2008).

Duteil, O., F. U. Schwarzkopf, C. W. Böning, and A. Oschlies (2014), Major role of the equatorial current system in setting oxygen levels in the eastern tropical Atlantic Ocean: A high-resolution model study, Geophys. Res. Lett., 41, 2033–2040, doi: 10.1002/2013GL058888.

Lachkar, Z., Orr, J. C., Dutay, J.-C., and Delecluse, P.: Effects of mesoscale eddies on global ocean distributions of CFC-11, CO2, and Δ14C, Ocean Sci., 3, 461-482, https://doi.org/10.5194/os-3-461-2007, 2007.

Lévy M. (2008) The Modulation of Biological Production by Oceanic Mesoscale Turbulence. In: Weiss J.B., Provenzale A. (eds) Transport and Mixing in Geophysical Flows. Lecture Notes in Physics, vol 744. Springer, Berlin, Heidelberg

McGillicuddy Jr, D. J. (2016). Mechanisms of physical-biological-biogeochemical interaction at the oceanic mesoscale. Annu. Rev. Mar. Sci., 8:1, 125-159, https://doi.org/10.1146/annurev-marine-010814-015606

Referee # 2

In this study the authors examine the anthropogenic CO_2 budget of the Arctic Ocean and how this inventory depends on model resolution. In that purpose they take advantage of the NEMO-v3.2 OGCM coupled to the biogeochemical model PISCES-v1. They perform experiments with three different horizontal resolution of the OGCM, namely 2°, 0.5°, and 0.25°. Inventories of anthropogenic carbon in the Arctic appear to increase with increasing resolution (from 2.0 to 2.6 Pg C). The role of air-sea fluxes and lateral transport in building these inventories is examined. In this model lateral transport accounts for 75% of the Arctic Ocean anthropogenic CO_2 inventory. A comparative study of the outputs of other modeling studies (CMIP5) allow concluding that models with larger lateral transport appear to better fit data-based estimates of the anthropogenic carbon in the Arctic Ocean. This partitioning does not depend on the model resolution. Resolution appears important in shaping the tracer distribution and improving data-model agreement.

The paper is well written and very well structured. However I have several concerns about the method and the way data-model comparison is performed. Before the method is thoroughly assessed this paper is not fit for publication.

Major comments

Reviewer Question 1 — I have serious concerns about the applied method for estimating the C_{ant}. Conclusions about the impact of model resolution might not be robust due to shortcoming in the method.

C_{ant} is rightly defined as the difference between the simulated historical and control ocean dissolved carbon contents. However, there is only one control experiment performed (page 5), that for ORCA05. As far as I understand the C_{ant} for ORCA2 and ORCA025 is evaluated as the difference between the respective 1958→2012 experiments and the ORCA05 control for the same period. Therefore I strongly suspect that the differences in CFC and C_{ant} among the different models may be explained by model drift. In order to lift that concern the following actions should be taken:

a. Perform control experiments over the period 1958→2012 for each model resolution.

b .While it is defensible to reduce the computation length with the high-resolution model (ORCA025) there is no such need for ORCA2, which runs even faster than ORCA05. The authors should also present results of historical and control experiments performed with ORCA2. The perturbation experiments should also be repeated with ORCA2.

The results of these additional experiments should then be compared to those presented in the present paper. This would provide a means of validating their method and assessing potential drifts

Reply:

a. We realize now that our original manuscript is woefully unclear about this point. We did not properly convey what was done. Indeed, each of our three resolutions already has its own control experiment over 1958-2012. For each resolution, C_{ant} was computed from two simulations (historical and control), both made at the same resolution. Therefore, there is no resolution-related drift issue. This

point will be clarified in section 2.2 of the revised manuscript.

b. As pointed out, we had already made a control simulation in ORCA2-PISCES from 1958 to 2012 although that was not clear in the submitted manuscript. For the same period, we have in addition added a C_{ant} perturbation simulation in ORCA2. Our strategy to consistently use the same ORCA05 output from the end of 1957 to initialize ORCA2 as well as ORCA025 in 1958 was by design. It produces a consistent set of results whereby the effect of resolution can be compared rigorously. Had we started all ORCA-PISCES simulations in 1870, which was not computationally feasible, there would have been larger differences due to resolution, e.g., based on the divergence shown in Figure 1. Hence the differences due to resolution discussed in the submitted manuscript are probably a lower limit, something that is clarified in the revised manuscript. In addition, for the revised manuscript, we made an additional C_{ant} perturbation simulation in ORCA2 initialized in 1765 (and 1870). That new simulation provides a more complete comparison with the analogous reference ORCA05 simulation as suggested by Referee #2.

Proposed change:

a. Both, the control and the historical simulations, were made for all three resolutions between 1958 to 2012 to correct potential model drifts. We defined the difference between the historical simulation and the control simulation as the anthropogenic component. ~~These~~ While the ORCA2 and ORCA025 simulations are presented for the first time, the ORCA05 simulations were ~~first~~ previously used by Bourgeois et al. (2016) to assess the budget of anthropogenic carbon in the coastal ocean. (page 5, lines 21–25 in the revised manuscript)

and

~~Thus with the same ORCA05 physical configuration, we made~~ To account for the missing carbon, we added the difference between two perturbation simulations, one ~~initialized~~ starting in 1765 (P1765) and the other one in 1870 (P1870). ~~Their difference is~~ For consistency, we applied the same initialization strategy as for the biogeochemical simulations, i.e. using ORCA05 until the end of 1957 with that output serving as the initial fields for subsequent 1958–2012 simulations in all three configurations. The difference of C_{ant} between P1765 and P1870 was later added to the NEMO-PISCES simulations, for each resolution separately. (page 6, lines 7–11, line 3 in the revised manuscript)

b. Lastly, we also made a perturbation simulation with using only ORCA2 from 1765 to 2012~~because the correction for that period is small; it is also less certain when applied to results from ORCA2 and ORCA025 given that it is based results from ORCA05. Thus it is not applied when discussing the effects of resolution,~~, which enables us to evaluate our simulation strategy, i.e. using ORCA05 until 1957 and then all three configurations from 1858 to 2012 (ORCA2, ORCA05, and ORCA025). (page 7, lines 1–3)

and

Meanwhile, we also consider that the simulated Arctic C_{ant} inventory in ORCA025 may well be too low because it was initialized with ORCA05 results in 1958. Had ORCA025 been initialed instead in 1765, which was not computationally feasible, its simulated inventory would probably be larger. Although we cannot assess this affect directly, we can do so indirectly by running tests at lower resolution and noting how trends differ between model resolutions after 1958. First, let us estimate how that same 1958 initialization affects the ORCA2 results, by taking the difference in simulated C_{ant} inventory between (1) the ORCA2 biogeochemical simulation from 1958 to 2012 initialized with ORCA05 in 1957 minus (2) the ORCA2 perturbation simulation from 1765 to 2012. That difference is −0.4 Pg C in 2005. Next

let us assume that there is a symmetry during 1765-2005 about the ORCA05 result with ORCA2 being lower and ORCA025 being higher as seen for the simulated period after 1958 (Figure ?? and Table ??). We infer then that ORCA025 Arctic C_{ant} inventory in 2005 would be ~0.4 Pg C larger had it been run initialized in 1765 rather than with the ORCA05 output in 1958. If so, the ORCA025 C_{ant} inventory in 2005 would increase from 2.6 to 3.0 Pg C, pushing it to closer to the center of the data-based range of 2.5–3.3 Pg C from [?]. After correcting both ORCA2 and ORCA025 for their 1958 initialization with ORCA05 output, the model range for the Arctic C_{ant} inventory would then be 1.6–3.0 Pg C in 2005, emphasizing even more the need to go beyond coarse-resolution models in the Arctic. (page 14, lines 13–26 in the revised manuscript)

and

At the same time, our highest resolution inventory is likely an underestimation as it was initialized in 1958 with ORCA05 results from 1765–1957. Details in model-data based comparison differ(page 18, lines 3–4 in the revised manuscript)

Reviewer Question 2 — The experiments, which are presented here are global. What would be the global figures for anthropogenic CO_2 uptake in the 5 cases? How do these figures compare to other assessments? Answering this request would allow evaluating whether the OGCMs as a whole would need serious refinements or should the effort concentrate on less-well resolved areas such as the Arctic Ocean.

Reply: The global corrected C_{ant} inventories for 1765-2008 for the three resolutions are given below as are the uncorrected inventories for 1870-2008 (in parentheses):

- ORCA2: 152 (127) Pg C
- ORCA05: 146 (121) Pg C
- ORCA025: 148 (124) Pg C

These corrections were made by adding the difference between the two tracers in the C_{ant} perturbation simulations, one initialized to zero in 1765 and the other in 1870, in each of the three resolutions. Those global perturbation results are as follows:

- ORCA2: 127 Pg C/153 Pg C
- ORCA05: 125 Pg C/150 Pg C
- ORCA025: 117 Pg C/142 Pg C

In the revised manuscript then, we present the corrected and uncorrected C_{ant} inventories for the biogeochemical simulations, plus the corrections from the perturbation simulations. Thus we show results for 9 cases rather than 5 because of the new perturbation simulations in ORCA2 and ORCA025 (4 additional cases since each has 2 perturbation tracers: one initialized in 1765 and the other in 1870, each again relying on ORCA05 until 1958) that were not provided in the previously submitted version of the manuscript. We also compare our results to the calculated corrections by Bronselaer et al. (2017).

Regarding other assessments, Khatiwala et al. (2009) report a data-based estimate for the global C_{ant} inventory for the period from 1765-2008 to be 140 ± 24 Pg C. For that same period, our results all lie within that range, falling near the upper boundary. Given the agreement of model results and

data-based estimates for the global ocean C_{ant} budget, it does not appear that further enhancements to resolution are needed to improve the global carbon budget. However, we would expect that improving resolution will have a large impact on some regional budgets, e.g., in zones where the ratio between the areas of shelf seas vs. open ocean is relatively large, such as in the Arctic Ocean. Inventories of anthropogenic carbon in regions with small areal extent will have little impact on the global inventory, but they do provide some indicator of the potential enhanced effect of ocean acidification in those regions. These results and concerns will be brought up in section 4.2 of the revised manuscript.

Proposed change:

~~The globally integrated increase in C_{ant} due to an earlier start date , as assessed with our two~~ Simulated global ocean C_{ant} inventories are 152 Pg C in ORCA2, 146 Pg C in ORCA05, and 148 Pg C in ORCA025 in 2008, all of which account for corrections for an earlier starting date from our perturbation simulations (~~P1765 – P1870), is 24~~P1765–P1870). The corrections are similar for each resolution, e.g., 24–25 Pg C in 1995, ~~an adjustment to the global inventory that is 17% lower than Bronselaer's~~ and are consistent with our biogeochemical model simulation strategy (all three resolutions initialized with the ORCA05 output in 1958). Furthermore, these model-based corrections are much like the 29 ± 5 Pg C correction calculated for the same 1765-1995 period with a data-based ~~assessment for a 1765 vs. 1850 start date.~~ approach Bronselaer et al. (2017) . For the 1765–2008 period, the data-based global C_{ant} inventory estimate from Khatiwala et al. (2009) is 140 ± 24 Pg C, the uncertainty range of which encompasses the results from all three model resolutions. (page 11, lines 17–23 in the revised manuscript)

and

To adequately model lateral ~~fluxes of C_{ant}~~ exchanges of C_{ant} in the Arctic Ocean, at least a resolution comparable to that used in ORCA05 may be needed, while resolutions comparable to that in ORCA025 or above may well be required to begin to capture the effects from density flows along the slope. As a consequence of the deficient representation of these density flows, we would expect to see an increase in C_{ant} when using even higher resolution. (page 16, lines 13–16 in the revised manuscript)

Reviewer Question 3 — The other main concern deals with the correction of data-based reconstructions of C_{ant} (Abstract, Sections 4.2 and 4.5, Fig. 9). The authors assume that reconstructed deep values of C_{ant} should be corrected downwards since observed CFC-12 concentrations at those depths are negligible. Doing so means overlooking the important fact that CFCs started to be emitted in the atmosphere much later than CO_2 .. Data-based estimates relying on the TTD method take into account the different tracer histories in the atmosphere. Clearly, the TTD method has limitations. The end-product displays rather large uncertainties. However, there are no sound arguments for setting the C_{ant} in the deep Arctic to zero.

Reply: Actually, there is some evidence that the GLODAPv2 estimate using the TTD method may overestimate C_{ant} concentrations in the deep Arctic Ocean. First, the water mass mean ages of deep and bottom waters are estimated to be about 250 to 300 years in the Eurasian basins (Nansen and Amundsen basins) and around 450 years in the Canadian basin (Makarov and Canada basins) (Tanhua et al., [2009]; Schlosser et al., [1994]). Thus one would expect very little if any C_{ant} would have reached those old deep waters. Second, the TTD method is known to estimate C_{ant} concentrations around 5 μmolkg^{-1} even when the CFC-12 concentrations approach zero (Waugh et al. [2006]), which demonstrates the lack of sensitivity and large uncertainty associated with the TTD estimates for older water masses. Given that data-based C_{ant} concentrations in the old, deep Arctic Ocean water masses

are 18% of surface concentrations while CFC-12 concentrations in the same deep water masses are only 3% of surface concentrations, it is plausible that the TTD method overestimates C_{ant}.

In the revised manuscript, we rephrased the text so as to indicate that to calculate the maximum potential error in the TTD-based estimate for the C_{ant} inventory in the Arctic, we set the deep TTD estimates to zero. In addition, we took out the reference to this estimation from the abstract and section 4.5.

Proposed change:

There are reasons to suspect that the GLODAPv2 estimate using the TTD method may overestimate C_{ant} in the deep Arctic. First, the water mass mean ages below 2000 m are shown to be of the order of 300 to 400 years (Tanhua et al., 2009; Schlosser et al., 1994) , older than the atmospheric CO_2 perturbation. Second, the TTD method estimates C_{ant} concentrations ($\sim$5 μmol kg^{-1}), even if the CFC-12 concentrations approach zero (Waugh et al., 2006) , which demonstrates the large uncertainty of the method when dealing with old water masses. To assess the maximum error associated with these potentially excessive deep TTD C_{ant} estimates, we recalculated the C_{ant} budget after zeroing out the C_{ant} below 2000 m~~, assuming that the actual concentrations of C_{ant} remain close to zero as suggested by the observed distribution of CFC-12, we can roughly estimate the effect on the basin-wide inventory by zeroing out those concentrations in the GLODAPv2 estimates (Lauvset et al., 2016) and recomputing the inventory~~. Doing so reduces the data-based inventory ~~in~~ of C_{ant} in the Arctic Ocean in 2002 by 10%. Applying the same 10% relative decrease to both the upper and lower limits of the data-based range from Tanhua et al. (2009) ~~reduces that to~~ leads to a minimum C_{ant} inventory of 2.2–~~3.0 PgC. That modified range brackets simulated inventories from both~~ 3.0 Pg C in 2005. Simulated inventories from both ORCA05 and ORCA025 are within this lower limit. (page 14, lines 4–12 in the revised manuscript)

and

When the CMIP5 models are compared to the corrected data-based estimate of the ~~C_{ant}~~ C_{ant} inventory (Sect. **??**), only the MIROC-ESM ~~and NorESM1-ME models with their inventories~~ with its inventory of 2.7 Pg C ~~and 2.4 Pg C fall within our simplistic revision of~~ fall within the data-based uncertainty estimate (~~2.2 to 3.0~~2.5 to 3.3 Pg C in 2005). Nearby ~~though is the~~ is the NorESM1-ME and HadGEM2-ES, which ~~falls~~ fall below the lower limit by ~~0.2~~0.1 and 0.5 Pg C, receptively. Further off are the MPI-ESM and GFDL-ESM models with their ~~C_{ant}~~ C_{ant} inventories in 2005 that are ~~0.6 to 1.2~~ 0.9 to 1.5 Pg C lower than the lower limit. The lowest estimates ~~though~~ are from both versions of the IPSL model whose inventories reach only ~~25~~$\sim$20% of the lower limit of our revised data-based range. Adjusting the CMIP5-model Arctic inventories upward by $\sim$0.4 Pg C to account for their late start date in 1850, as we did for our three simulations, would place ~~three~~ two of them (MIROC-ESM, and NorESM1-ME~~, and HadGEM2-ES~~) above the lower boundary of our revised data-based uncertainty estimate, and HadGEM2-ES just 0.1 Pg C below this lower boundary. (page 16, lines 22–30 in the revised manuscript)

and

We replaced as well the corrected estimate by the uncorrected estimate in Figure 9.

Reviewer Question 4 — Modeled CFC-12 inventories in the Arctic (Fig. 5 and page 12, lines 24 and 25) appear to be much lower than the observed ones, even with ORCA25. Would it be possible to provide total (integrated over depth and distance) inventories along the AOS94 and Beringia 2005 expedition pathways and compare the 3 model results to the data inventories? The low CFC inventory provides an indication that low C_{ant} would be expected too.

Reply: Excellent suggestion. Thank you. We have now calculated these total inventories integrated over depth and distance along sections:

- Beringia 2005
  - Observations: 9.4 μmol m^{-1}
  - ORCA025: 7.7 μmol m^{-1}
  - ORCA05: 5.8 μmol m^{-1}
  - ORCA2: 3.7 μmol m^{-1}
- AOS94
  - Observations: 5.5 μmol m^{-1}
  - ORCA025 : 4.8 μmol m^{-1}
  - ORCA05 : 3.5 μmol m^{-1}
  - ORCA2 : 2.0 μmol m^{-1}

For both expeditions, the observed CFC-12 section inventories are underestimated by 13-18% in ORCA05, 31-38% in ORCA05, and 61-64% in ORCA2. This tendency with resolution for these section inventories is consistent with that seen for the Arctic Ocean's basin-wide inventory where the data-based estimate is underestimated by 13-15% in ORCA025, 22-24% in ORCA05, and 34-36% in ORCA2.

Proposed change: Lastly, we calculate CFC-12 inventories along the two sections, integrated over depth and distance (Table 6). Depending on the expedition, ORCA025 underestimates the observed CFC-12 section inventories by 13-18%, ORCA05 by 31-38%, and ORCA2 by 61-64%. (page 11, lines 13–15)

and

A table (table 6) of these integrated values is added.

Reviewer Question 5 — In addition, a description of how CFC-12 is modeled is lacking.

Reply: Details about how CFC-12 was simulated is included in the Methods section of the revised manuscript.

Proposed change: CFC-12 is a purely anthropogenic tracer, a sparingly soluble gas whose concentration began to increase in the atmosphere in the early 1930's, part of which has been transferred to the ocean via air-sea gas exchange. Its uptake and redistribution in the ocean has been simulated following OCMIP-2 protocols (Dutay et al., 2002) . The CFC-12 flux (F_{CFC}) at the air-sea interface was calculated as follows:

$$F_{CFC} = k_w(\alpha_{CFC}\ p\mathrm{CFC} - C_s)(1 - I), \tag{1}$$

where k_w is the gas-transfer velocity (piston velocity) in m s^{-1} (Wanninkhof, 1992) , pCFC the atmospheric partial pressure of CFC-12 in atm from the reconstructed atmospheric history by Bullister (2015) , C_s is the sea surface concentration of CFC-12 (mol m^{-3}), α_{CFC} is the solubility of CFC-12 (mol m^{-3}atm^{-1}) from Warner and Weiss (1985) , and I is the model's fractional sea-ice cover. Once

in the ocean, CFC-12 is an inert tracer that is distributed by advection and diffusion; it has no internal sources and sinks. Many high-precision measurements of CFC-12 are available throughout the ocean, in sharp contrast to C_{ant} which cannot be measured directly. (page 7, lines 5–21 in the revised manuscript)

Minor comments

Reviewer Question 6 — Abstract, line 10: C_{ant} is not defined yet.

Reply: C_{ant} is defined in line 5.

Reviewer Question 7 — Page 3, line 2: a reference to the figure displaying the map of the Arctic should be made here; the reader does not necessarily know about the area characteristics. In this sense Fig. 2 should become Fig. 1.

Reply: The revised manuscript includes these suggested changes.

Reviewer Question 8 — Page 3, line 2: "The bathymetry of the Arctic Ocean differs from that of the in other other oceans..."

Reply: In the revised manuscript we changed "of the in other other" to "in other".

Reviewer Question 9 — Page 3, line 25: is 'laminar' right?

Reply: Yes, "laminar" is a common term used to describe coarse-resolution ocean models. See for example Penduff et al (2011).

Reviewer Question 10 — Page 4, line 2: table 3 does not come into order.

Reply: In the revised manuscript, that table is put in order.

Reviewer Question 11 — Page 4, lines 11 and 12: "NEMO uses partial steps so that the model better matches the observed topography. Thus the depth of the deepest cell can be smaller than the original grid cell." Could you develop or reformulate? It is hard to understand what it is meant here.

Reply: We propose to rephrase the sentence as follows: "NEMO uses the partial-step approach for the model to better match the observed topography. In this approach, the bathymetry of the model is not tied directly to the bottom edge of the deepest ocean grid level, which varies with latitude and longitude; rather, the deepest ocean grid level for each column of grid cells is partially filled in to better match the observed ocean bathymetry."

Reviewer Question 12 — Page 4, line 22: there is no mention of the Si:P and Fe:P ratios.

Reply: The Fe:C and Chl:C ratios of both phytoplankton groups as well as the Si:C ratio of diatoms are predicted prognostically by PISCES. These model details are mentioned in the revised manuscript.

Reviewer Question 13 — Page 4, line 29: does sediment mobilization only intervene in the Fe cycle? Or does it also affect the other nutrients?

Reply: Yes, sediment mobilization only intervenes in the Fe cycle, a point that is clarified in the revised manuscript.

Reviewer Question 14 — Page 4, line 30: "... following the lead of Moore et al. (2004)."

Reply: That phrase was changed to "following Moore et al. (2004).".

Reviewer Question 15 — Page 5, line 33: "... simulations made in with the same circulation model..."

Reply: In that sentence, "in with" was changed to "with".

Reviewer Question 16 — Pages 5 and 6: the many occurrences of 'xCO_2 ' should be changed into 'CO_2 '.

Reply: To avoid any confusion, we prefer to explicitly refer to 'xCO_2 ', namely the atmospheric mixing ratio or mole fraction of CO_2 , i.e., the number of moles of CO_2 per mole of air. That ratio is typically multiplied by 10^6 and given in ppmv (or simply ppm) because CO_2 is a trace gas in the atmosphere. In the text, we need to distinguish between xCO_2 and the partial pressure of CO_2 (pCO_2), which always has pressure units (μatm). Although these two quantities are often confused, they are not the same and our method depends on keeping them straight.

Reviewer Question 17 — Page 6, equation (1): what are the units of pCO_2 and T?

Reply: The units of pCO_2 [μatm] and T [°C] are indicated in the revised manuscript

Reviewer Question 18 — Page 6, line 25: "given that it is based on results from ORCA05."

Reply: This above-mentioned phrase was part of a paragraph that will be removed in the revised version of manuscript. That paragraph explains how the biogeochemical simulations (all three resolutions) were corrected using the ORCA05 C_{ant} perturbation runs. Now with our complete set of C_{ant} perturbation simulations, two C_{ant} perturbation tracers in each of the three resolutions as detailed earlier, this explanation is unnecessary.

Reviewer Question 19 — Page 6, line 28: reference to Table 4 should appear here.

Reply: This line is also part of the paragraph that is removed in the revised manuscript.

Reviewer Question 20 — Page 10, line 24: "apparent in ORCA025 6)."

Reply: The "6)" is changed to "(Figure 6)".

Reviewer Question 21 — Page 12, line 22: "that that excess simulated CFC-12 between 1000 and 2000 m..."

Reply: The double that is changed to that.

Reviewer Question 22 — Tables do not come into order. Table 3 should become Table 1, Table 1→2, and Table 2→3.

Reply: Tables are ordered correctly in the revised manuscript.

Reviewer Question 23 — Table 1: the 'b' subscript does not appear anywhere in the table

Reply: The 'b' subscript is added to Table 1 in the revised manuscript.

Reviewer Question 24 — Table 2, caption: "Fitted parameters for the perturbation approach for the tracers starting in 1765 (P1765) and in 1870 (P1870)."

Reply: In the revised manuscript, this sentence is changed to "Fitted parameters for the perturbation simulations P1765 and P1870."

Reviewer Question 25 — Table 4: what do exactly represent the lines "Total transport" and "Summed lateral flux"?

Reply: Both are changed to 'Sum' in the revised manuscript. Both terms represent the sum of the lateral fluxes: in one case it is the lateral water flux and in the other the lateral C_{ant} flux.

Reviewer Question 26 — Table 4, caption: "Simulated values are calculated for the same time period as observations."

Reply: This text is revised as proposed by the Referee.

Reviewer Question 27 — Fig. 1 and Fig. 2 should be inverted

Reply: These figures are inverted in the revised manuscript.

Reviewer Question 28 — Fig. 10, caption: The first sentence "Profiles of Ω_A after the early industrial period period simulated only in ORCA05 (1870–1957), after intializing the other models in 1958." is confusing. I suggest to remove most of it; it is not needed.

Reviewer Question 29 — "Results are shown for ORCA05 in 1960 (black solid) as well as for ORCA2 (green dot- dash), ORCA05 (red dashes), and ORCA025 (blue dots) in 2012."

Reply: In the revised manuscript, both sentences are simplified and combined: "Profiles of Ω_{arag} for ORCA05 in 1960 (black solid) as well as ORCA2 (green dot-dash), ORCA05 (red dashes), and ORCA025 (blue dots) in 2012."

References

Penduff, T., M. Juza, B. Barnier, J. Zika, W.K. Dewar, A. Treguier, J. Molines, and N. Audiffren, 2011: Sea Level Expression of Intrinsic and Forced Ocean Variabilities at Interannual Time Scales. J. Climate, 24, 5652–5670, https://doi.org/10.1175/JCLI-D-11-00077.1

Schlosser, P., Kromer, B., Östlund, G., Ekwurzel, B., Bönisch, G., Loosli, H., and Purtschert, R. (1994). On the 14C and 39Ar Distribution in the Central Arctic Ocean: Implications for Deep Water Formation. Radiocarbon, 36(3), 327-343. doi:10.1017/S003382220001451X

Tanhua, T., E. P. Jones, E. Jeansson, S. Jutterstrm̈, W. M. Smethie Jr., D. W. R. Wallace, and L. G. Anderson (2009), Ventilation of the Arctic Ocean: Mean ages and inventories of anthropogenic CO2 and CFC-11, J. Geophys. Res., 114, C01002, doi: 10.1029/2008JC004868.

Waugh, D. W., Hall, T. M., McNeil, B. I., Key, R. and Matear, R. J. (2006), Anthropogenic CO2 in the oceans estimated using transit time distributions. Tellus B, 58: 376-389. doi:10.1111/j.1600-0889.2006.00222.x

Model constraints on the anthropogenic carbon budget of the Arctic Ocean

Jens Terhaar[1], James C. Orr[1], Marion Gehlen[1], Christian Ethé[2], and Laurent Bopp[3]

[1]Laboratoire des Sciences du Climat et de l'Environnement, LSCE/IPSL, CEA-CNRS-UVSQ, Université Paris-Saclay, 91191 Gif-sur-Yvette, France
[2]Institut Pierre et Simon Laplace, 4 Place Jussieu, 75005 Paris, France
[3]LMD/IPSL, Ecole Normale Supérieure / PSL Research University, CNRS, Ecole Polytechnique, Sorbonne Université, Paris, France

Correspondence to: Jens Terhaar (jens.terhaar@lsce.ipsl.fr)

Abstract. The Arctic Ocean is projected to experience not only amplified climate change but also amplified ocean acidification. Modeling future acidification depends on our ability to simulate baseline conditions and changes over the industrial era. Such centennial-scale changes require a global model to account for exchange between the Arctic and surrounding regions. Yet the coarse resolution of typical global models may poorly resolve that exchange as well as critical features of Arctic Ocean circulation. Here we assess how simulations of Arctic Ocean storage of anthropogenic carbon (~~C_{ant}~~ C_{ant}), the main driver of open-ocean acidification, differ when moving from coarse to ~~eddy-admitting~~ eddy-admitting resolution in a global ocean circulation-biogeochemistry model (NEMO-PISCES). The Arctic's regional storage of ~~C_{ant}~~ C_{ant} is enhanced as model resolution increases. While the coarse-resolution model configuration ORCA2 (2°) stores 2.0 Pg C in the Arctic Ocean between 1765 and 2005, the eddy-admitting versions ORCA05 and ORCA025 (1/2° and 1/4°) store 2.4 and 2.6 Pg C. ~~That result from ORCA025~~ The difference in inventory between model resolutions is only due to their divergence after 1958. It would be larger had all model resolutions been initialized in 1765 as was the intermediate resolution model (ORCA05). The ORCA25 results falls within the uncertainty range from a previous data-based ~~C_{ant}~~ C_{ant} storage estimate (2.5 to 3.3 Pg C). ~~Yet those limits may each need to be reduced by about 10% because data-based C_{ant} concentrations in deep waters remain at $\sim$6 μmol kg^{-1}, while they should be almost negligible by analogy to the near-zero observed CFC-12 concentrations from which they are calculated.~~ Across the three resolutions, there was roughly three times as much ~~anthropogenic carbon~~ C_{ant} that entered the Arctic Ocean through lateral transport than via the flux of CO_2 across the air-sea interface. Wider comparison to nine earth system models that participated in the Coupled Model Intercomparison Project Phase 5 (CMIP5) reveals much larger diversity of stored ~~anthropogenic carbon~~ C_{ant} and lateral transport. Only the CMIP5 models with higher lateral transport obtain ~~C_{ant}~~ C_{ant} inventories that are close to the data-based estimates. Increasing resolution also enhances acidification, e.g., with greater shoaling of the Arctic's average depth of the aragonite saturation horizon during 1960–2012, from 50 m in ORCA2 to 210 m in ORCA025. To assess the potential to further refine modeled estimates of the Arctic Ocean's ~~C_{ant}~~ C_{ant} storage and acidification, sensitivity tests that adjust model parameters are needed given that century-scale global ocean biogeochemical simulations still cannot be run routinely at high resolution.

1 Introduction

The Arctic is experiencing amplified ocean acidification (Steinacher et al., 2009) and amplified climate change (Bekryaev et al., 2010), both of which may ~~have consequences on~~ affect the marine ecosystem (Gattuso and Hansson, 2011). The main driver of the ongoing acidification of the open ocean is the increase in atmospheric CO_2 during the industrial era and the ensuing uptake of anthropogenic carbon from the atmosphere. Although this absorbed anthropogenic carbon cannot be measured directly, being dominated by the natural component, it has been estimated from other oceanographic data. For instance, Gruber et al. (1996) developed the $\Delta C^\star$ method, building on seminal studies (Brewer, 1978; Chen and Millero, 1979) and their criticism (Broecker et al., 1985) as well as large new global data sets with improved CO_2 system measurements. That back-calculation method first calculates the total dissolved inorganic carbon (C_T) at equilibrium with atmosphere before the water parcel is subducted. That preformed C_T is then corrected for changes due to biological activity, as estimated from measurements of dissolved oxygen, total alkalinity (A_T), and nutrients, after which an estimate of preindustrial carbon is removed, finally yielding $\Delta C^\star$. ~~In the high latitudes though, the~~ Yet the $\Delta C^\star$ method's assumption of a constant air-sea CO_2 disequilibrium appears problematic in the high latitudes (Orr et al., 2001). A second approach approximates the invasion of anthropogenic CO_2 into the interior ocean by a Transient Time Distribution (TTD) method, itself constrained by observations of transient-tracers such as CFC-12 or SF_6 (Hall et al., 2002; Waugh et al., 2004). A third approach uses a Green's function instead of a TTD while also exploiting multiple transient tracers to assess the ocean's temporally changing distribution of anthropogenic carbon (Khatiwala et al., 2009). A comparison of these methods suggests that by 2010 the ocean had absorbed 155 ± 31 Pg C of anthropogenic carbon, around one-third of all emitted anthropogenic carbon (Khatiwala et al., 2013)

Less attention has been paid to anthropogenic carbon storage in the Arctic. Sabine et al. (2004) estimated that the Arctic Ocean had absorbed 4.9 Pg C by 1994. Yet without estimates for anthropogenic carbon in the Arctic itself, Sabine et al. scaled the Arctic inventory to be 5% of their $\Delta C^\star$-based estimate for global anthropogenic carbon storage, assuming the same Arctic:Global ocean ratio as in the global gridded distribution of observed CFC-12 (Willey et al., 2004). More recently, Tanhua et al. (2009) used Arctic observations of CFC-11, CFC-12, and SF_6 and the TTD approach, revising the former Arctic anthropogenic carbon storage estimate downward to a range of 2.5 to 3.3 Pg C for year 2005. With that estimate, they emphasized that while the Arctic Ocean represents only 1% of the global ocean volume, it stores 2% of the global ocean's anthropogenic carbon. Although these numbers are relatively small, Arctic concentrations of anthropogenic C_T must be relatively large, thus driving enhanced acidification in the Arctic Ocean.

To provide an alternate approach to estimate anthropogenic carbon in the Arctic and to assess its budget and the mechanisms that control it, we made carbon cycle simulations over the industrial era using a coupled ocean circulation-biogeochemical model. A global-scale configuration is used to account for the Arctic in the context of the global carbon cycle, while avoiding artifacts from lateral boundary conditions that are needed for regional models. Simulations with the same model (NEMO-PISCES) are made at three resolutions, from coarse to eddy admitting, to help assess the extent to which coarse-resolution models may need to be improved to adequately simulate anthropogenic carbon storage in the Arctic Ocean.

Coarse resolution may be insufficient to adequately represent Arctic Ocean bathymetry, shelf, slopes, and ridges, all of which affect Arctic Ocean circulation (Rudels et al., 1994). The bathymetry of the Arctic Ocean differs from that in other ~~other~~ oceans in part because of the preponderance of shelf seas, comprising 53% of the total surface area (Jakobsson, 2002) (Figure 1). The remaining 47% of the surface area covers 95% of the total volume of the Arctic Ocean, split across four deep basins: the Nansen basin, the Amundsen basin, the Makarov basin, and the Canadian basin. Water masses enter these deep basins (1) via deep inflow from the Atlantic through the Fram Strait into the Nansen basin, (2) via deep-water inflow from the Barents Sea to the Nansen basin through the St Anna Trough, as cooling increases density, (3) and via density flows along the continental shelves that are driven by brine rejection from sea-ice formation (Jones et al., 1995). These three local processes are difficult to resolve in coarse-resolution models, e.g., local density flows necessitate much higher resolution (Proshutinsky et al., 2016). Model resolution also affects the simulated interior circulation of the Arctic Ocean by its connection to the global ocean circulation via four relatively narrow and shallow passages: (1) the Canadian Archipelago, (2) the Fram Strait, (3) the Barents Sea Opening and (4) the Bering Strait (Aksenov et al., 2016). Lateral exchange of water, carbon, and nutrients across these sections also affects Arctic Ocean primary production and acidification (Popova et al., 2013; Luo et al., 2016).

Here we use a three-dimensional model to help refine the estimate of the total anthropogenic carbon in the Arctic Ocean while assessing the dominant pathways by which anthropogenic carbon enters the Arctic Ocean and the relative importance of that lateral input relative to the air-sea flux. Three simulations made at increasingly higher grid resolution allow us to assess the extent to which the coarse resolution used by typical global ocean models may need to be improved to adequately estimate storage of anthropogenic carbon in the Arctic Ocean and associated ocean acidification.

2 Methods

2.1 Models

For our study, we ~~use~~ used the global ocean circulation model NEMO-v3.2 (Nucleus for European Modeling of the Ocean - version 3.2) including ~~its~~ the biogeochemical component PISCES-v1 (Pelagic Interactions Scheme for Carbon and Ecosystem Studies) (Aumont and Bopp, 2006). The NEMO model has three parts: (1) the ocean dynamics and thermodynamics model OPA (Madec, 2008), (2) the sea-ice model LIM (Vancoppenolle et al., 2009), and (3) the passive tracer module TOP. This physical model is coupled via TOP to version 1 of PISCES. ~~In~~ For this study we ~~use~~ used NEMO at three resolutions: a laminar 2°-configuration (ORCA2) typical of coarse-resolution ocean models (Madec et al., 1998), which does not resolve eddies; an intermediate 0.5°-configuration (ORCA05) that just begins to allow eddies to appear spontaneously (Bourgeois et al., 2016); and a higher-resolution, eddy admitting version, i.e., 0.25°-configuration (ORCA025), which is still not eddy resolving (Barnier et al., 2006). All three configurations have a tripolar, curvilinear horizontal grid. One grid pole (singularity) is located at the geographical South Pole while the conventional North-Pole grid singularity over the Arctic Ocean has been replaced by two singularities, both displaced over land, one over Canada and the other over Russia (Madec et al., 1998), thereby saving computational costs and avoiding numerical artifacts.

From 90°S to 20°N, the grid is a normal Mercator grid; north of 20°N, it is distorted into ellipses to create the two northern singularities (Barnier et al., 2006; Madec, 2008). The grid size changes depending on resolution and location (Table 1). The mean horizontal grid size in the Arctic Ocean (average length of the 4 horizontal edges of surface grid cells in the Arctic Ocean) is 121 km in ORCA2, 29 km in ORCA05, and 14 km in ORCA025. The minimum horizontal grid size in the Arctic is 63 km in ORCA2, 9 km in ORCA05, and 3 km in ORCA025. Vertically, all three model configurations have the same discretization, where the full-depth water column is divided into 46 depths levels, whose thicknesses increase from 6 m at the surface to 500 m in the deepest grid box. For ~~ocean~~ its bathymetry, the ocean model relies on the 2-minute bathymetry file ETOPO2 from the National Geophysical Data Center~~is used~~, which is based on satellite derived data (Smith and Sandwell, 1997) except for the highest latitudes: the IBCAO bathymetric data is used in the Arctic (Jakobsson et al., 2000) and BEDMAP bathymetric data is used for the Southern Ocean south of 72°S (Lythe and Vaughan, 2001). To interpolate the bathymetry on the model grid, the median of all data points in one model grid cell was computed. NEMO uses ~~partial steps so that the model better matches~~ the partial-step approach for the model to better match the observed topography. ~~Thus the depth of the deepest cell can be smaller than the original grid cell~~In this approach, the bathymetry of the model is not tied directly to the bottom edge of the deepest ocean grid level, which varies with latitude and longitude; rather, the deepest ocean grid level for each column of grid cells is partially filled in to better match the observed ocean bathymetry. For the parameter values and numerical characteristics of the ORCA025 configuration, we ~~follow~~ followed Barnier et al. (2006). The lateral isopycnal diffusion and viscosity coefficients ~~are then~~ were chosen depending on the resolution (Table 2). ~~Note that~~ In ORCA2, a Laplacian viscosity operator ~~is usedin ORCA2~~was used, whereas a bi-Laplacian operator ~~is~~ was used in ORCA05 and ORCA025. To simulate the effect of eddies on the mean advective transport in the two coarser resolution configurations, the eddy parameterization scheme of Gent and Mcwilliams (1990) was applied with eddy diffusion coefficients indicated in Table 2.

The biogeochemical model PISCES (Aumont and Bopp, 2006) includes four plankton functional types: two phytoplankton (nanophytoplankton and diatoms) and two zooplankton (micro- and meso-zooplankton). The growth of phytoplankton is limited by the availability of five nutrients: nitrate, ammonium, total dissolved inorganic phosphorus P_T, total dissolved silicon Si_T, and iron. The nanophytoplankton and diatoms are distinguished by their need for all nutrients, with only diatoms requiring silicon. ~~In the living compartments, the~~ While the Fe:C and Chl:C ratios of both phytoplankton groups as well as the Si:C ratio of diatoms are predicted prognostically by PISCES, the remaining macronutrient ratios are held constant at C:N:P = 122:16:1 (Takahashi et al., 1985). The same ratio holds for nonliving compartments: dissolved organic matter (DOM) and both small and large sinking particles, which differ in their sinking velocity. In PISCES, nutrients are supplied by three external pathways: atmospheric dust deposition, river delivery, and sediment mobilization of iron. Dust deposition ~~is~~ was taken from a simulation by Tegen and Fung (1995). River discharge of C_T and dissolved organic carbon (DOC) is based on the Global Erosion Model (GEM) by Ludwig et al. (1998). Riverine DOC ~~is~~ was assumed to be labile, being transformed into C_T as soon as it enters the ocean. River delivery of the other four nutrients (Fe, N, P, and Si) ~~are~~ were calculated from C_T, assuming constant ratios of C:N:P:Si:Fe = 320:16:1:53.3:3.64$\times 10^{-3}$ (Meybeck, 1982). For sediment mobilization, dissolved iron input was parameterized as 2 μmol Fe m^{-2} day^{-1} for depths shallower than 1100 m following ~~the lead of~~ Moore et al. (2004).

2.2 Biogeochemical simulations

For initial conditions, we used observational climatologies for temperature and salinity combined from three sources (Barnier et al., 2006), for dissolved oxygen and nutrients (nitrate, P_T, and Si_{T}) from the 2001 World Ocean Atlas (Conkright et al., 2002), and for preindustrial C_{T} and A_{T} from the observation-based Global Data Analysis Product (GLODAP) (Key et al., 2004). As comparable observational climatologies for DOC and iron are lacking, those variables were initialized from output of a 3000-year spin up of an ORCA2 simulation including PISCES. Other tracers have short recycling times and ~~thus were initalized~~ were thus initialized with globally uniform constants.

For physical boundary conditions, all simulations ~~are~~ were forced with the same DRAKKAR Forcing Set (DFS) constructed by Brodeau et al. (2010). This historical reanalysis data set provides surface air temperature and humidity at 2 m, wind fields at 10 m, shortwave and longwave radiation, and the net surface freshwater flux (evaporation minus precipitation). This data set covers 55 years, including 1958–2001 from version 4.2 and then 2002–2012 from version 4.4.

A 50-year spin up was first made from rest in the ORCA05 NEMO-PISCES model (coupled circulation-biogeochemistry), after initializing the model variables with the above-mentioned fields. The resulting simulated physical and biogeochemical fields were then used to initialize the ORCA05 NEMO-PISCES simulations, and that model was subsequently integrated during 1870-1957. Since no atmospheric reanalysis is available during that period, we simply ~~loop~~ looped the DRAKKAR Forcing Set. Then at the beginning of 1958, the ORCA05 simulated fields were interpolated to the ORCA2 and ORCA025 grids, and simulations were continued in each of the three configurations during 1958 to 2012 (Fig. 2).

For this study we made two types of simulations, historical and control, both forced with the same reanalysis fields. In addition, the control ~~simulation is~~ simulations were forced with the preindustrial CO_2 concentration of 287 ppm in the atmosphere over the entire period from 1870 to 2012. The historical ~~simulation is~~ simulations were forced with yearly averaged historical atmospheric CO_2 concentrations reconstructed from ice cores and atmospheric records over 1870 to 2012 (Le Quéré et al., 2015). ~~We define~~ Both, the control and the historical simulations, were made for all three resolutions between 1958 to 2012 to correct potential model drifts. We defined the difference between the historical simulation and the control simulation as the anthropogenic component. ~~These~~ While the ORCA2 and ORCA025 simulations are presented for the first time, the ORCA05 simulations were ~~first~~ previously used by Bourgeois et al. (2016) to assess the budget of anthropogenic carbon in the coastal ocean.

2.3 ~~Perturbation~~ C_{ant} perturbation simulation

Because of computational limitations, it was necessary to start the anthropogenic CO_2 perturbation of our reference ORCA05-PISCES simulation in 1870 as opposed to the traditional earlier reference of 1765 (Sarmiento et al., 1992), a more realistic approximation of the start of the industrial-era CO_2 increase. A similar compromise was adopted for CMIP5 (Taylor et al., 2012). During that missing 105 years, atmospheric xCO_2 increased from 277.86 to 287.29 ppm, a 9 ppm difference that seems small relative to today's total perturbation with atmospheric xCO_2 now above 400 ppm. However, Bronselaer et al. (2017) estimated that global ocean uptake of ~~C_{ant}~~ C_{ant} in 1995 is actually underestimated by ~30% (29 Pg C) for simulations that

reference the natural preindustrial state to 1850 rather than 1765. The cause is partly due to carbon uptake during the missing 1765–1850 period, but mostly it is due to the higher preindustrial reference for atmospheric xCO_2 that results in the air-sea flux of ~~C_{ant}~~ C_{ant} being underestimated throughout the entire simulation. Unfortunately, we cannot use Bronselaer et al.'s results to correct our biogeochemical simulations because their reference date in the mid 19th century is 20 years earlier than ours and because they do not include the Arctic Ocean in their global data-based assessment.

Instead, to correct ~~results from~~ for the late starting date of our biogeochemical simulations, we ~~essentially add in the difference between two additional simulations made in the same circulation model but coupled to the~~ made additional simulations using the more efficient single-tracer perturbation approach (Sarmiento et al., 1992) rather than the full PISCES biogeochemical model (24 tracers). ~~By definition, the perturbation tracer is initialized to zero everywhere; it accounts for only the perturbation (C_{ant}), assuming it is independent of the natural carboncycle. Thus with the same ORCA05 physical configuration, we made~~ To account for the missing carbon, we added the difference between two perturbation simulations, one ~~initialized~~ starting in 1765 (P1765) and the other one in 1870 (P1870). ~~Their difference is~~ For consistency, we applied the same initialization strategy as for the biogeochemical simulations, i.e. using ORCA05 until the end of 1957 with that output serving as the initial fields for subsequent 1958–2012 simulations in all three configurations. The difference of C_{ant} between P1765 and P1870 was later added to the NEMO-PISCES simulations, for each resolution separately.

The perturbation approach of Sarmiento et al. (1992) avoids the computationally intensive standard CO_2 system calculations by only accounting for the perturbation (C_{ant}), assuming it is independent of the natural carbon cycle. By focusing only on anthropogenic carbon~~and exploiting~~, this approach exploits a linear relationship between the anthropogenic change in oceanic pCO_2 [μatm] and its ratio with the ocean's corresponding change in C_T (~~C_{ant}~~ C_{ant}):

$$\frac{\delta pCO_{2_{oc}}}{C_{ant}} \frac{\delta pCO_{2_o}}{C_{ant}} = z_0 + z_1 \delta pCO_{2_{oc_o}}, \tag{1}$$

where ~~$\delta pCO_{2_{oc}}$~~ δpCO_{2_o} is the perturbation in oceanic ~~pCO_2~~ pCO_2 and the coefficients z_0 and z_1 are each quadratic functions of temperature [°C],

$$z_0 = a_0 + a_1 T + a_2 T^2 \tag{2}$$

$$z_1 = b_0 + b_1 T + b_2 T^2. \tag{3}$$

In the model, Eq. (1) ~~is~~ was rearranged to solve for surface-ocean ~~$\delta pCO_{2_{oc}}$~~ δpCO_{2_o} in terms of ~~C_{ant}~~ C_{ant} (Sarmiento et al., 1992, Eq. (11)), as needed to compute the air-sea flux (Sarmiento et al., 1992, Eq. (2)). In the air-sea flux equation, the atmospheric xCO_2 ~~is~~ was corrected for humidity and atmospheric pressure to convert to $pCO_{2_{atm}}$. The atmospheric xCO_2 history for 1765–1869 is from Meinshausen et al. (2017), while the history for 1870 and beyond is the same as used in the NEMO-PISCES simulations. One set of coefficients was derived for our reference atmospheric xCO_2 in 1765; another set was derived for our reference atmospheric xCO_2 in 1870 (Table 3). The original approach was only updated to use the equilibrium constants recommended for best practices (Dickson et al., 2007) and to cover a perturbation of up to 280 ppm (see Supplement). The relative error introduced by approximating the perturbation to the ocean CO_2 system equilibria with Eq. (1) remains less than $\pm 0.3\%$ across the global ocean's observed temperature range when ~~$\delta pCO_2^{oc} < 280$~~ $\delta pCO_2^{oc} < 280$ ppm.

To correct our biogeochemical simulations for the late starting date, we ~~use~~ used the time-varying difference in ~~C_{ant}~~ C_{ant} for every grid cell between the two perturbation simulations (P1765 – P1870), adding that to the ~~C_{ant}~~ C_{ant} simulated in the biogeochemical simulations. ~~That late-start-date correction is applied to all model output when computing the total C_{ant} inventories and the vertical C_{ant} profiles (Sects. 3.3 and 4.2). On the other hand, that correction is not applied when the focus is on differences between 1960 and~~

Lastly, we also made a perturbation simulation with using only ORCA2 from 1765 to 2012~~because the correction for that period is small; it is also less certain when applied to results from ORCA2 and ORCA025 given that it is based results from ORCA05. Thus it is not applied when discussing the effects of resolution.~~, which enables us to evaluate our simulation strategy, i.e. using ORCA05 until 1957 and then all three configurations from 1858 to 2012 (ORCA2, ORCA05, and ORCA025).

2.4 CFC-12 simulation

CFC-12 is a purely anthropogenic tracer, a sparingly soluble gas whose concentration began to increase in the atmosphere in the early 1930's, part of which has been transferred to the ocean via air-sea gas exchange. Its uptake and redistribution in the ocean has been simulated following OCMIP-2 protocols (Dutay et al., 2002). The CFC-12 flux (F_{CFC}) at the air-sea interface was calculated as follows:

$$F_{CFC} = k_w(\alpha_{CFC}\, p\mathrm{CFC} - C_s)(1 - I), \tag{4}$$

where k_w is the ~~1960-2012 budget, lateral fluxes, nor changes in the aragonite saturation horizon during that time (Sects. 3.4, 4.3, 4.4, and 4.6). To illustrate the generally second-order effect of this correction on for instance the lateral fluxes of C_{ant}, results from both perturbation simulations are tabulated alongside those from the biogeochemical simulations~~gas-transfer velocity (piston velocity) in m s^{-1} (Wanninkhof, 1992), pCFC the atmospheric partial pressure of CFC-12 in atm from the reconstructed atmospheric history by Bullister (2015), C_s is the sea surface concentration of CFC-12 (mol m^{-3}), α_{CFC} is the solubility of CFC-12 (mol m^{-3}atm^{-1}) from Warner and Weiss (1985), and I is the model's fractional sea-ice cover. Once in the ocean, CFC-12 is an inert tracer that is distributed by advection and diffusion; it has no internal sources and sinks. Many high-precision measurements of CFC-12 are available throughout the ocean, in sharp contrast to C_{ant} which cannot be measured directly.

2.5 Arctic Ocean

To assess the anthropogenic carbon budget in the Arctic Ocean, we ~~adopted~~ adopt the regional domain defined by Bates and Mathis (2009) (Fig. 1). That domain's lateral boundaries and the volume of water contained within them vary slightly among the three model versions due to their different resolutions and bathymetries ~~.~~(Table 1). The signature of these different volumes is also apparent in the integrated quantity of anthropogenic carbon that is stored in the Arctic in 1958, ~~even though~~ although the fields for all three models are based on the same 1957 field from the ORCA05 model (Fig. 2).

2.6 Transport across boundaries

Transects ~~were~~ are defined (Fig. 1) along the four boundaries as consistently as possible for the three resolutions. Water transport across each of the four boundaries ~~was~~ is calculated for each model configuration by using monthly average water velocities at each boundary grid cell along a transect multiplied by the corresponding area of the face of the grid cell through which the water flows. For boundaries defined by a row of cells (Fram Strait, Canadian Arctic Archipelago [CAA], and Bering Strait), the transport ~~was~~ is calculated across the northern face of each cell. Conversely, for the boundary that is a jagged line (Barents Sea Opening), for each cell the transport ~~was~~ is calculated at the northern and eastern faces of each cell and the two transports are summed. Then for each transect, transport across all of its cells are summed to obtain the transect's monthly net transport. For the ~~C_{ant}~~ C_{ant} transport, we ~~did~~ do the same but also ~~multiplied~~ multiply the water transport at the boundary between two grid cells with their volume-weighted monthly-average concentration. This multiplication of monthly means introduces an error into the transport calculation owing to neglect of shorter term variability. To shed light on that error, we ~~summed~~ sum results from those monthly calculations across all four sections, ~~integrated~~ integrate them over time from 1960 to 2012, and ~~compared~~ compare that to the net transport of ~~C_{ant}~~ C_{ant} into the Arctic Ocean implied by the inventory change minus the cumulative air-sea flux over the same time period. The inventory of ~~C_{ant}~~ C_{ant} is the total mass of ~~C_{ant}~~ C_{ant} inside the Arctic Ocean at a given time, while the cumulative flux is the time-integrated air-sea flux of anthropogenic CO_2 over the Arctic Ocean since the beginning of the simulation. The difference between these two spatially integrated values is the reference value for the net lateral flux into the Arctic Ocean to which is compared the less exact total lateral flux of anthropogenic carbon computed from monthly mean velocity and concentration fields integrated over time. The relative error for transport of C_{ant} across the separate boundaries introduced by the monthly average calculations is ~~27~~28% for ORCA2, 7% for ORCA05, and ~~4~~3% for ORCA025. Note that this error applies neither to the C_{ant} inventory, nor to the cumulative air-sea flux or the lateral fluxes, which are all calculated 'online', during the simulations.

2.7 CFC-12 observational data

Model simulations were evaluated indirectly by comparing simulated to observed CFC-12. We choose CFC-12 to evaluate the model, because it is an anthropogenic, passive, conservative, and inert tracer, and in contrast to anthropogenic carbon, it is directly measurable. The CFC-12 atmospheric concentration increased from zero in the 1930s to its peak in the 2000s, since declining as a result of the Montreal protocol. Thus CFC-12 is a transient tracer similar to anthropogenic carbon but for which there exist extensive direct measurements, all carried out with high precision during WOCE (World Ocean Circulation Experiment) and CLIVAR (Climate and Ocean - Variability, Predictability and Change) era. Nowadays, ocean models are often evaluated with CFC-11 or CFC-12, especially those destined to be used to assess anthropogenic carbon uptake ~~(?Orr et al., 2017)~~(Dutay et al., 2002; Orr et al., 2017).

The CFC-12 observations used in this study come from two trans-Arctic cruises: the 1994 Arctic Ocean Section (AOS94) (Jones et al., 2007) and the Beringia 2005 expedition (Anderson et al., 2011) (Fig. 1). AOS94 started on 24 July and finished on 1 September, during which CFC-12 measurements were made at 39 stations. That section starts in the Bering Strait, enters

the Canada basin adjacent to Mendeleev ridge, continues to the Makarov basin, and ends at the boundary of the Nansen basin and the Barents Sea. The Beringia expedition started on 19 August and ended on 25 September 2005. It started off the coast of Alaska, went through the Canada and Makarov basins, crossed the Lomonosov ridge, and its last CFC-12 station was taken on the Gakkel ridge. These two cruises were chosen among other cruises because of their geographically similar placement and because they cross large parts of the Arctic, including almost all four major basins.

2.8 Data-based estimates of anthropogenic carbon

Our simulated ~~C_{ant}~~ $\tilde{C}_{ant}$ was compared to data-based estimates from Tanhua et al. (2009) for the year 2005 and from GLODAPv2 for the year 2002 (Lauvset et al., 2016), both based on the TTD approach.

3 Results

3.1 Physical Evaluation

3.1.1 Lateral water fluxes

The lateral water flux across each the four Arctic boundaries is a fundamental reference for the simulated physical transport, especially when the goal is to construct a budget that includes lateral transport of passive tracers. Results for lateral water transport in the three model resolutions may be grouped into two classes: coarse resolution and higher resolutions. In ORCA2, water enters the Arctic Ocean from Barents Sea and the Bering Strait (2.1 Sv split evenly), with 86% of that total leaving the Arctic via the Fram Strait and the remaining 14% flowing out via the CAA (Table 4). Conversely, outflow through the CAA is seven times larger for ORCA05 and nine times larger for ORCA025, being fueled by 26% to 46% more inflow via the Bering Strait and 110% to 170% more inflow via the Barents Sea. Outflow via the Fram Strait is 1.76 Sv in ORCA2, 1.42–1.75 Sv in ORCA05, and 1.46–1.80 Sv in ORCA025, depending on the time period (Table 4).

Relative to the observed CAA outflow of 2.7 Sv (Curry et al., 2014; Straneo and Saucier, 2008), only ORCA05 and ORCA025 simulate similar results. In contrast, ORCA2's simulated CAA outflow is about one ninth of that observed. Likewise, its inflow via the Barents Sea is half of that observed, while the two higher resolution simulations have Barents Sea inflows that are 20% and 40% larger than observed. Yet for inflow through the Bering Strait, it is ORCA2 that is closest to the observed estimate, overestimating it by 30%, while ORCA05 and ORCA025 overestimate it by 60% and 90%. Thus too much Pacific water appears to be entering the Arctic Ocean. All resolutions underestimate the central observational estimate for the Fram Strait outflow by $\sim$12% but still easily fall within the large associated uncertainty range. Summing up, the net water transport across all four boundaries is not zero. A net outflow between 0.12 and 0.17 Sv is found for the three model resolutions owing to river inflow and precipitation as well as artifacts caused by using monthly averages. In contrast, when the observed water transport estimates at all four boundaries are summed up, there is a net outflow of 1.9 Sv, more than ten times larger. This strong net outflow is also much larger than freshwater input from rivers (0.08 Sv) (McClelland et al., 2006) and precipitation (0.12 Sv) (Yang, 1999). It can only be explained by uncertainties in the data-based estimates of water transport,

which are at least ± 2.7 Sv for the net transport based on the limited uncertainties available for transport across the individual boundaries (Table 4). The excessive central observational estimated for the net outflow might be explained by a data-based estimate for the Barents Sea inflow that is too weak combined with a data-based estimate for the Fram Strait outflow that is too strong, a possibility that is consistent with results from the higher resolution models ORCA05 and ORCA025.

3.1.2 Sea ice

Because sea-ice cover affects the air-sea CO_2 flux and hence anthropogenic carbon concentrations in the ocean, we compare the modeled sea-ice cover to that observed by the U.S. National Snow and Ice Data Center (Walsh et al., 2015). Yearly averages of sea-ice extent are quite similar between the observations and models. Only in summer are simulated sea-ice concentrations slightly too high (by 0.25–0.5 $\times$ 10^6 km^3). Despite this overall agreement in integrated sea-ice extent, regional differences are larger. During winter (Fig. 3), all three model configurations marginally overestimate the sea-ice extent northeast of Iceland and north of the Labrador Sea, while the simulated sea-ice extent in the Barents Sea and the Bering Strait are similar to observations. During summer, the simulated sea-ice extent resembles that observed in the eastern Arctic particularly near the Atlantic, but all model resolutions overestimate sea-ice extent north of the Kara Sea, the Laptev Sea, and the East Siberian Sea. This overestimation should reduce air-sea CO_2 fluxes locally in these regions. The close model-data agreement for sea-ice extent in terms of the total amount, its trend and seasonal coverage, as well as regional coverage in winter contrasts with the tendency of the models to overpredict sea-ice cover in summer in the highest latitudes of the eastern Arctic.

3.1.3 Atlantic water

In the Arctic Ocean, water temperature is used to help identify water masses, with values above 0°C typically coming from the Atlantic Ocean (Woodgate, 2013). The observed temperature along the 1994 and 2005 sections (Fig. 4) indicates that Atlantic Water (AW) is found between 200 and 1000 m, penetrating laterally below the strongly stratified Arctic Ocean surface waters. In ORCA025, this AW layer is deeper and more diffuse, lying between 500 and 1500 m, thus leading to a cold bias around 500 m and a warm bias around 1000 m. The Beringia station at the boundary between the Barents Sea and the Nansen basin indicates AW lies between 200 m (2.5°C) and the seafloor at 1000 m (0°C). Conversely in the same location in ORCA025, model temperatures remain above 1.5°C throughout the water column. That lower maximum temperature and weaker vertical gradient suggests that when ORCA025's Atlantic water enters the Arctic Ocean through the Barents Sea it is too diffuse, being well mixed throughout the water column. Weaker maxima in the simulated temperature relative to observations are also found further west in the Canada basin along both sections. There observed temperatures reach maxima of 1.1°C, while ORCA025's maxima reach only 0.5°C.

The other two resolutions represent Atlantic water circulation more poorly than does ORCA025. Both simulations show water with temperatures higher than 0°C only at the southern end of the Nansen basin. Vertically, these water masses are situated around 400 m for ORCA2 and between 200 and 1300 m for ORCA05.

3.2 CFC-12

Simulated CFC-12 was compared among the three resolutions and with observations, focusing first on basin-scale tendencies based on vertical profiles of the distance-weighted means along the 2005 section (Fig. 5). That comparison reveals that among resolutions, simulated CFC-12 concentrations differ most between 400 ~~m and 2000~~and 1900 m; conversely, above and below that intermediate zone, simulated average profiles are nearly insensitive to resolution~~both above and below that intermediate zone. In those intermediate waters~~ . In that intermediate zone and above, simulated concentrations are also generally lower than observed. The only ~~exceptions are (1)~~ exception is the top 100 m of the Canada basin where all resolutions overestimate observed values by 10%~~and (2) between~~ . Between 200 and 400 m all resolutions underestimate observations by ∼50%. Below 400 m, the ORCA2 CFC-12 concentrations decline quickly to zero (∼1000~~and 2000 m in the Canada and Makarov basins where the~~ m), while the ORCA05 and ORCA025 ~~model overpredicts observations~~ concentrations continue to increase both being by 15% greater at 900 m. Below that depth, the ORCA05 concentrations decline quickly reaching zero at 1350 m, while ORCA025 concentrations remain above 1 pmol kg^{-1} until 1400 m. Between 1100 and 1500 m, average CFC-12 concentrations along the section in ORCA025 are larger than observed by up to ~~40% . Conversely, lower resolution generally implies lower and less realistic simulated~~ ∼10% at 1300 m. This overestimation of CFC-12 ~~concentrations in the intermediate zone. Below 2000~~by ORCA025 reaches up to 40% in the Canada and Makarov basins. Below 1900 m, the simulated concentrations are essentially zero, while the observations are ~~only~~ slightly higher (0.12 pmol kg^{-1}). For comparison, the reported detection limit for CFC-12 for the Beringia 2005 expedition is 0.02 pmol kg^{-1} (Anderson et al., 2011). ~~The general shape of profiles also differs. While the observations exhibit a generally smooth decline down to about 1500 m, the models show a steeper reduction down to about 300 m and then much weaker gradients down to 1500 m. While ORCA2 tends to decline quickly at first, ORCA05 generally remains nearly vertical, and ORCA025 actually even increases with depth in the Canada and Makarov basins.~~

Given the closer overall agreement of the ORCA025 simulated CFC-12 ~~simulation with~~ to the observations, let us ~~zoom in to compare its details to observations~~ now focus on its evaluation along the 1994 and 2005 sections (Fig. 6). On the Atlantic end of the Beringia 2005 section, where water enters the Nansen basin from the Barents Sea, the water column in ORCA025 appears too well mixed, having CFC-12 concentrations that remain above 2.0 pmol kg^{-1}. Conversely, observed CFC-12 is less uniform, varying from 2.8 pmol kg^{-1} at the surface to 1.3 pmol kg^{-1} in bottom waters at 1000 m, thereby indicating greater stratification. The same contrast in stratification was deduced from modeled and observed temperature profiles at the same location (Sect. 3.1.3). On the other side of the Arctic in the Canada basin, there are observed local chimneys of CFC-12 where concentrations remain at about 2.0 pmol kg^{-1} from near the surface down to 1000 m, particularly ~~in~~ along the 1994 section. These chimneys suggest localized mixing that is only barely apparent in ORCA025 (Fig. 6). Such localized features are absent at lower resolution.

Lastly, we calculate CFC-12 inventories along the two sections, integrated over depth and distance (Table 6). Depending on the expedition, ORCA025 underestimates the observed CFC-12 section inventories by 13-18%, ORCA05 by 31-38%, and ORCA2 by 61-64%.

3.3 Anthropogenic carbon inventories and concentrations

~~The globally integrated increase in C_{ant} due to an earlier start date , as assessed with our two~~ Simulated global ocean C_{ant} inventories are 152 Pg C in ORCA2, 146 Pg C in ORCA05, and 148 Pg C in ORCA025 in 2008, all of which account for corrections for an earlier starting date from our perturbation simulations (~~P1765 – P1870), is 24~~P1765–P1870). The corrections are similar for each resolution, e.g., 24–25 Pg C in 1995, ~~an adjustment to the global inventory that is 17% lower than Bronselaer et al.'s~~ and are consistent with our biogeochemical model simulation strategy (all three resolutions initialized with the ORCA05 output in 1958). Furthermore, these model-based corrections are much like the 29 ± 5 Pg C correction calculated for the same 1765-1995 period with a data-based ~~assessment for a 1765 vs. 1850 start date.~~ approach (Bronselaer et al., 2017). For the 1765–2008 period, the data-based global C_{ant} inventory estimate from (Khatiwala et al., 2009) is 140 ± 24 Pg C, the uncertainty range of which encompasses the results from all three model resolutions.

In the Arctic Ocean, ~~which is absent from the data-based assessment, there was a corresponding simulated basin-wide increase of 0.4~~the corrected modeled C_{ant} inventories range from 1.9 to 2.5 Pg C in ~~2005.~~

~~The simulated~~ 2002 and from 2.0 to 2.6 Pg C in 2005 (from ORCA2 to ORCA025). These simulated basin-wide ~~storage (inventory)of simulated C_{ant}, adjusted for the late starting date, was~~ Arctic Ocean C_{ant} inventories were compared to the TTD-based estimates of anthropogenic carbon from (1) the GLODAPv2 assessment (Lauvset et al., 2016) normalized to the year 2002 and (2) the Tanhua et al. (2009) assessment normalized to 2005. ~~These~~ The data-based ~~estimates suggest~~ assessment from GLODAPv2 suggests that 2.9 Pg C of anthropogenic carbon was stored in the Arctic Ocean in 2002~~while~~ , while that from Tanhua et al. suggests that 2.5–3.3 Pg C was stored there in 2005. ~~The adjusted modeled C_{ant} inventory in~~ In 2002~~ranges from 1.9 to 2.5 Pg C (from ORCA2 to ORCA025)~~, the upper ~~end of which~~ limit of the of the modeled C_{ant} inventory range remains 0.4 Pg C lower than the GLODAPv2 data-based estimate. In 2005, the ~~modeled range is slightly higher (2.0 to 2.6 Pg C) with the upper end from ORCA025 falling~~ upper limit of the model range falls just within the data-based uncertainty range of Tanhua et al. (2009).

~~These model-data~~ As for the global estimates, the Arctic Ocean C_{ant} inventories include corrections for the late starting date of the biogeochemical simulations. These correction is 0.4 Pg C in 2005 for each resolution (Table 5).

The differences in basin-wide ~~inventories were investigated further~~ inventory estimates were further studied by comparing vertical profiles of ~~C_{ant}~~ C_{ant} from the models to those from the GLODAPv2 data-based estimates (Fig. 7). Surface concentrations in ORCA05 and ORCA025 are up ~35% larger (+12 µmol kg^{-1}) than the data-based estimate, whereas the ORCA2 concentration is ~22% larger (+7 µmol kg^{-1}). ~~Diving deeper~~Moving downward, by 150 m the simulated concentrations in all resolutions ~~drop~~ have dropped below the data-based estimates and remain so, except for ORCA025, down to the ocean bottom. ~~At~~ Data-model differences are largest at 400 m~~the difference is largest~~, with all resolutions underestimating data-based estimates by up to ~28% (9 µmol kg^{-1}). Below ~~400 m~~that depth, results from the three resolutions differ more. The ORCA2 ~~C_{ant}~~ C_{ant} concentration decreases monotonically to 11 µmol kg^{-1} at 1000 m and to 0 µmol kg^{-1} at 2300 m. In ORCA05, concentrations decrease slowly to 19 µmol kg^{-1} at 1000 m, below which they decrease rapidly, essentially to 0 µmol kg^{-1} at 2300 m. Only ORCA025 increases again below 400 m, reaching a local maximum in ~~C_{ant}~~ C_{ant} at 900 m, an increase that causes the

ORCA025 results to exceed data-based estimates by up to 2 µmol kg^{-1} (~11%) at 1100 m. Below 1500 m, ORCA025 concentrations decline quickly, essentially reaching zero at 2300 m. Conversely, data-based anthropogenic carbon concentrations remain at roughly a constant 6 µmol kg^{-1} all the way down to the seafloor. The main differences between ORCA025 and data-based estimates are thus found in the deep Arctic Ocean below 1600 m. An analogous simulated local maximum and the underestimation near 400 m was also seen for CFC-12 (Fig. 5). ~~Unlike for C_{ant} though~~Yet unlike for C_{ant}, CFC-12 results differ below 2000 m, where observed CFC-12 concentrations are proportionally much smaller than those above.

3.4 Anthropogenic carbon budget

We calculated the budget for ~~C_{ant}~~ C_{ant} from 1960 to 2012 (Tables 4 and 5). During this period, the ~~C_{ant}~~ C_{ant} inventory in ORCA025 increased by ~~1.91~~1.98 Pg C, 80% of which is stored in the four major Arctic ~~Oceans~~ Ocean basins: the Nansen Basin (~~0.29~~0.30 Pg C), the Amundsen Basin (~~0.33~~0.34 Pg C), the Makarov Basin (~~0.32~~0.33 Pg C) and the Canada Basin (~~0.57~~0.61 Pg C). Although the Canada Basin ~~C_{ant}~~ C_{ant} inventory increased most, its volume is larger so that its average ~~C_{ant}~~ C_{ant} concentration increased less than in the other basins (Fig. 7). Out of the total inventory stored in the Arctic Ocean during these five decades, about one-fourth (~~0.47~~0.48 Pg C) entered the Arctic Ocean via air-sea flux, most of which was transferred from atmosphere through the surface of the Barents Sea (Fig. 8). The remaining 75% (~~1.45~~1.50 Pg C) entered the Arctic Ocean via lateral transport. This net lateral influx is the sum of the fluxes (1) from the Atlantic through the Fram Strait (~~0.04~~ 0.06 Pg C), (2) from the Atlantic to the Barents Sea (~~1.70~~1.98 Pg C), (3) from the Pacific through the Bering Strait (~~0.89~~1.03 Pg C) and (4) to the Atlantic via the CAA (~~-1.25~~-1.50 Pg C). Summed up, the net ~~inflow~~ lateral inflow of carbon across the four boundaries is ~~1.39~~1.45 Pg C. This lateral flux computed from monthly mean ~~C_{ant}~~ C_{ant} concentrations and flow fields is ~~0.06~~0.05 Pg C (~~4%~~) 3%) is smaller than the lateral flux computed from the change in inventory minus the cumulative air-sea flux (Fig. 8). Within the Arctic, coastal regions typically exhibit net lateral losses, while the deep basins exhibit net lateral gain. The largest lateral loss occurs in the Barents Sea, where the cumulative air-sea flux of ~~C_{ant}~~ C_{ant} is also largest (Fig. 8).

The budget of ~~C_{ant}~~ C_{ant} changes notably with resolution. Higher resolution results in more simulated ~~C_{ant}~~ C_{ant} being stored in the Arctic region, with increases in both the cumulative air-sea flux and lateral transport. The ~~C_{ant}~~ C_{ant} inventory change from 1960 to 2012 nearly doubles with the resolution increase between ORCA2 and ORCA025 (from ~~1.04 to 1.91~~1.08 to 1.98 Pg C). Out of that additional ~~C_{ant}~~ C_{ant}, 93% is found between 300 and 2200 m with the maximum being located at 1140 m. The remaining 7% is located between the surface and 300 m (Fig. 7). Besides these differences in the vertical partitioning of stored ~~C_{ant}~~ C_{ant}, resolution also affects regional partitioning of ~~C_{ant}~~ C_{ant} (Figs. 7 and 8). When refining resolution from ORCA2 to ORCA05, the Arctic Ocean ~~C_{ant}~~ C_{ant} inventory increases by ~~0.46~~0.47 Pg C, 72% of which occurs in the two Eurasian basins: the Nansen (0.19 Pg C) and Amundsen (~~0.14~~0.15 Pg C) basins. Another ~~24~~23% of that increase occurs in the two Amerasian basins: the Makarov (0.06 Pg C) and Canada (0.05 Pg C) basins. Coastal regions account for only ~~4~~5% of the total inventory increase. In contrast, the subsequent resolution enhancement between ORCA05 and ORCA025 results in little increase in inventory in the Eurasian basins (~~0.02~~0.03 Pg C) but much more in the Amerasian basins (~~0.35~~0.37 Pg C).

As resolution is refined between ORCA2 and ORCA025, the Arctic ~~C_{ant}~~ C_{ant} inventory increases as a result of a ~~62~~66% increase in the air-sea flux (+~~0.18~~0.19 Pg C) and a ~~93~~90% increase in the lateral flux (+~~0.70~~0.71 Pg C). Thus the relative

contribution of the lateral flux increases from ~~72~~73% to 76%. Changing model resolution also affects the pathways by which ~~C_{ant}~~ C_{ant} enters the Arctic Ocean (Table 4). The most prominent change occurs in the CAA. From ORCA2 to ORCA025, the net outflow of ~~C_{ant}~~ C_{ant} through the CAA increases sevenfold (from ~~-0.18 to -1.25~~ -0.22 to -1.50 Pg C). Other notable changes include (1) the net transport through the Fram Strait declining from a sizable ~~net outflow~~ (-0.59 Pg C) to a slight net ~~inflow~~ ~~(0.04~~outflow (-0.06 Pg C), (2) the inflow through the Barents Sea increasing by 150% (from ~~0.68 to 1.70~~0.79 to 1.98 Pg C), and (3) the inflow of ~~C_{ant}~~ C_{ant} through the Bering Strait increasing by ~~40~~39% (from ~~0.64 to 0.89~~0.74 to 1.03 Pg C).

4 Discussion

4.1 CFC-12

The simulated CFC-12 in ORCA025 underestimates observed concentrations between 100 and ~~1000~~1100 m, overestimates them between ~~1000 and 2000~~1100 and 1500 m, and ~~closely matches~~ again underestimates the low observed concentrations below ~~2000~~1500 m. Temperature sections suggest that ~~that~~ excess simulated CFC-12 between ~~1000 and 2000~~1100 and 1500 m is due to a vertical displacement of inflowing Atlantic water, which descends too deeply into the Arctic (Fig. 4). Such vertical displacement would indeed reduce simulated CFC-12 concentrations above 1000 m and enhance them between ~~1000 and 2000~~1100 and 1500 m. Yet the underestimation of integrated CFC-12 mass above ~~1000~~1100 m is larger than the overestimation below ~~1000~~1100 m. Thus vertical displacement of Atlantic water cannot provide a full explanation. Simulated CFC-12 concentrations above ~~1000~~1100 m could also be too low because ventilation of subsurface waters is probably too weak, an hypothesis that is consistent with the simulated vertical gradients in both temperature and CFC-12 that are too strong between 100 and ~~1000~~1100 m.

4.2 Anthropogenic carbon

Relative to CFC-12, simulated deep ~~C_{ant}~~ C_{ant} in ORCA025 underestimates observational estimates ~~of C_{ant}~~ by proportionally much more. Both tracers have similarly shaped profiles, but the data-based ~~C_{ant}~~ C_{ant} profile differs from the observed CFC-12 profile below 1500 m. Above 1000 m, ORCA025 underestimates data-based estimates of ~~C_{ant}~~ C_{ant} as well as observed CFC-12 owing to weak ventilation in the model. Between 1000 and ~~2000~~1500 m, simulated ~~C_{ant}~~ C_{ant} and CFC-12 in ORCA025 are higher than data-based and observed concentrations. The local maxima for simulated CFC-12 and ~~C_{ant}~~ C_{ant} in that depth range can be explained by the excessively deep penetration of simulated Atlantic water masses, which are rich in both tracers.

Below ~~1500~~2000 m, simulated ~~C_{ant}~~ C_{ant} largely underestimates data-based estimates. ~~These~~ The data-based ~~C_{ant}~~ C_{ant} concentrations remain higher than those simulated, with an offset of $\sim$6 μmol kg^{-1} from 2000 m to the ocean floor (~~amounting to~~ 18% of the surface concentration), while observed CFC-12 concentrations are ~~close to those simulated~~relatively closer to zero, dropping to 0.1 pmol kg^{-1} below 2000 m (~~amounting to~~ 3% of the surface concentration). Hence the data-based estimates of ~~C_{ant}~~ C_{ant}, which are not measured directly, appear to be too large below ~~1500~~2000 m in the Arctic Ocean. ~~Below~~

There are reasons to suspect that the GLODAPv2 estimate using the TTD method may overestimate C_{ant} in the deep Arctic. First, the water mass mean ages below 2000 m are shown to be of the order of 300 to 400 years (Tanhua et al., 2009; Schlosser et al., 1994), older than the atmospheric CO_2 perturbation. Second, the TTD method estimates C_{ant} concentrations ($\sim$5 μmol kg^{-1}), even if the CFC-12 concentrations approach zero (Waugh et al., 2006), which demonstrates the large uncertainty of the method when dealing with old water masses. To assess the maximum error associated with these potentially excessive deep TTD C_{ant} estimates, we recalculated the C_{ant} budget after zeroing out the C_{ant} below 2000 m~~, assuming that the actual concentrations of C_{ant} remain close to zero as suggested by the observed distribution of CFC-12, we can roughly estimate the effect on the basin-wide inventory by zeroing out those concentrations in the GLODAPv2 estimates (Lauvset et al., 2016) and recomputing the inventory~~. Doing so reduces the data-based inventory ~~in~~ of C_{ant} in the Arctic Ocean in 2002 by 10%. Applying the same 10% relative decrease to both the upper and lower limits of the data-based range from Tanhua et al. (2009) ~~reduces that to~~ leads to a minimum C_{ant} inventory of 2.2–~~3.0 PgC. That modified range brackets simulated inventories from both~~ 3.0 Pg C in 2005. Simulated inventories from both ORCA05 and ORCA025 are within this lower limit.

Meanwhile, we also consider that the simulated Arctic C_{ant} inventory in ORCA025 may well be too low because it was initialized with ORCA05 results in 1958. Had ORCA025 been initialed instead in 1765, which was not computationally feasible, its simulated inventory would probably be larger. Although we cannot assess this affect directly, we can do so indirectly by running tests at lower resolution and noting how trends differ between model resolutions after 1958. First, let us estimate how that same 1958 initialization affects the ORCA2 results, by taking the difference in simulated C_{ant} inventory between (1) the ORCA2 biogeochemical simulation from 1958 to 2012 initialized with ORCA05 in 1957 minus (2) the ORCA2 perturbation simulation from 1765 to 2012. That difference is $-$0.4 Pg C in 2005. Next let us assume that there is a symmetry during 1765-2005 about the ORCA05 result with ORCA2 being lower and ORCA025 being higher as seen for the simulated period after 1958 (Figure 2 and Table 5). We infer then that ORCA025 Arctic C_{ant} inventory in 2005 would be $\sim$0.4 Pg C larger had it been run initialized in 1765 rather than with the ORCA05 output in 1958. If so, the ORCA025 C_{ant} inventory in 2005 would increase from 2.6 to 3.0 Pg C, pushing it to closer to the center of the data-based range of 2.5–3.3 Pg C from Tanhua et al. (2009). After correcting both ORCA2 and ORCA025 for their 1958 initialization with ORCA05 output, the model range for the Arctic C_{ant} inventory would then be 1.6–3.0 Pg C in 2005, emphasizing even more the need to go beyond coarse-resolution models in the Arctic.

4.3 Lateral flux

In our model, about three-fourths of the net total mass of ~~C_{ant}~~ C_{ant} that accumulates in the Arctic Ocean enters laterally from the Atlantic and Pacific Oceans, independent of model resolution. Our simulated lateral fluxes of ~~C_{ant}~~ C_{ant} were compared to data-based estimates from studies that multiply ~~C_{ant}~~ C_{ant} concentrations (TTD data-based estimates) along the Arctic boundaries by corresponding observation-based estimates of water transport.

The simulated lateral transport of ~~C_{ant}~~ C_{ant} in ORCA025 generally agrees with data-based estimates within ~~the latter's~~ their large uncertainties. These uncertainties result from uncertainties in data-based estimates of ~~C_{ant}~~ C_{ant} and from uncertainties in observational constraints on water flow, which also varies interannually (Jeansson et al., 2011). For the Fram Strait, Jeansson

et al. (2011) estimated a net ~~C_{ant}~~ C_{ant} outflux (from the Arctic) of 1 ± 17 Tg C yr^{-1} in 2002, while for 2012 Stöven et al. (2016) estimate an outflux of 12 Tg C yr^{-1} but without uncertainties. For the same years, ORCA025 simulates a net outflux of ~~6~~8 Tg C yr^{-1} in 2002 but a net influx (to the Arctic) of ~~7~~5 Tg C yr^{-1} in 2012. Both model and data-based estimates vary greatly between 2002 and 2012. Across the Barents Sea Opening, there is a consistent net influx from the Atlantic to the Arctic Ocean, i.e., 41 ± 8 Tg C yr^{-1} in 2002 for the data-based estimate (Jeansson et al., 2011) and (~~44~~50 Tg C yr^{-1}) for ORCA025.

More recently, Olsen et al. (2015) added data-based estimates of lateral fluxes at the two other major Arctic Ocean boundaries, completing the set of four that define the perimeter. They estimate an inflow of ~18 Tg C yr^{-1} from the Pacific through the Bering Strait and an outflow through the CAA of ~29 Tg C yr^{-1}, both for the 2000s. For the same time period, ORCA025 simulates ~~one-third~~ one-half more inflow through the Bering Strait (~~24~~27 Tg C yr^{-1}) and ~~7~~24% more outflow through the CAA (~~31~~36 Tg C yr^{-1}). The larger Bering-Strait ~~C_{ant}~~ C_{ant} inflow in ORCA025 is consistent with its overestimated Bering-Strait water inflow (Table 4, Section 3.1.1). Integrating over all four lateral boundaries, Olsen et al. found a total net ~~C_{ant}~~ C_{ant} influx of ~29 Tg C yr^{-1}, which is ~~22~~24% less than that simulated in ORCA025 (~~37~~38 Tg C yr^{-1}). Olsen et al. did not provide uncertainties, but the uncertainty of their net lateral flux estimate is at least $\pm$18 Tg C yr^{-1} based on the data-based transport estimates at the two other Arctic boundary sections where uncertainties are available (Table 4).

~~Although the simulated and data-based lateral fluxes generally agree within available uncertainties, results for the former are not corrected for the 1870 start date of the biogeochemical simulations. Correcting to a 1765 start date would increase the magnitude of the simulated lateral fluxes by 10% to 20% based on our ORCA05 perturbation simulations (compare P1765 to P1870 in Table 5). However, that correction may depend on resolution. In any case, we expect it will remain much smaller than the differences due to resolution.~~

Weighing in at about one-third of the lateral flux is the simulated air-sea flux of ~~C_{ant}~~ C_{ant} in ORCA025 of 10 Tg C yr^{-1} in 2005. That simulated estimate is only about 40% of the data-based estimate of 26 Tg C yr^{-1} from Olsen et al. (2015). Although no uncertainty is provided with that data-based air-sea flux estimate, it too must be at least $\pm$18 Tg C yr^{-1} given that it is calculated as the difference between the data-based storage estimate (Tanhua et al., 2009) and Olsen et al.'s data-based net lateral flux. ~~Given that large uncertainty , the modeled and data-based estimates of the~~ The simulated air-sea ~~flux are not statistically different~~flux falls within that assigned uncertainty range for the data-based estimate. In any case, both the model and data-based estimates suggest that the air-sea flux plays a minor role in the anthropogenic carbon budget of the Arctic Ocean, respectively representing 24 and 47% of the total ~~C_{ant}~~ C_{ant} input. For both, the lateral flux dominates.

4.4 Model Resolution

Basin inventories of anthropogenic carbon differ because of how resolution affects their volume, bathymetry, circulation patterns, and source waters. Much of the water in the Nansen and Amundsen basins has entered laterally from the Atlantic Ocean through the Fram Strait and the Barents Sea (Jones et al., 1995). Water inflow through the Barents Sea increases by 150% when changing from ORCA2 to ORCA05 but only by 20% more between ORCA05 and ORCA025. Water inflow in those two higher resolution models is also closer to observational estimates. ~~Furthermore, the~~ With increasing water inflow, the inflow of C_{ant} is also increased. Although more C_{ant} is entering the Arctic Ocean, the air-sea C_{ant} flux into the Arctic Ocean increases with

resolution. This apparent contradiction can be explained by two mechanism: (1) Higher resolution increases the inflow of C_{ant} through the Fram Strait, which is mainly occurring in subsurface currents and therefore does not substantially impact surface C_{ant} concentrations nor hence air-sea exchanges of C_{ant} and (2) higher resolution enhances deep-water formation, mainly in the Barents Sea, which reduces surface C_{ant} and thus enhances the air-to-sea flux of C_{ant}. Although the air-sea flux increases slightly, the larger lateral water fluxes in ORCA05 and ORCA025 ~~largely~~ mainly explain their higher ~~C_{ant}~~ C_{ant} concentrations in the Nansen and Amundsen basins. Some of this inflowing water continues to flow further along the slope, across the Lomonosov ridge into the Makarov basin, and then across the Mendeleev ridge into the Canada basin. Yet how well models simulate that flow path depends on lateral resolution. Between ORCA2 and ORCA05, basin ~~C_{ant}~~ C_{ant} inventories increase by ~~17~~16% in the Canada basin (+0.05 Pg C) and by ~~43~~40% the Makarov basin (+0.06 Pg C). But between ORCA05 to ORCA025, increases are two to four times greater: +~~0.23~~0.25 Pg C in the Canada basin and +0.12 Pg C in the Makarov basin (Sect. 3.4). The change from ORCA2 to ORCA05 seems to mainly improve lateral exchanges with adjacent oceans, while the change from ORCA05 to ORCA025 improves inner-Arctic Ocean circulation.

As ~~this increase~~ the increase from ORCA05 to ORCA025 stems from finer, more realistic representation of lateral transport within the Arctic, it would appear that eddying ocean models may be needed to adequately simulate the interior circulation in terms of its effect on ~~C_{ant}~~ C_{ant} storage in the Arctic Ocean. In the Canada basin~~though~~, such lateral inflow may not be the only source of ~~C_{ant}~~ C_{ant}. Another major source appears to come from density flows along the continental slope, driven by brine rejection from sea-ice formation over the continental shelves (Jones et al., 1995). A signature of this source in the observed sections may be the chimneys of constant CFC-12 concentration from the surface to about 1000 m in the Canada basin, features for which only ORCA025 exhibits any such signature, albeit faint. To adequately model lateral ~~fluxes of C_{ant}~~ exchanges of C_{ant} in the Arctic Ocean, at least a resolution comparable to that used in ORCA05 may be needed, while resolutions comparable to that in ORCA025 or above may well be required to begin to capture the effects from density flows along the slope. As a consequence of the deficient representation of these density flows, we would expect to see an increase in C_{ant} when using even higher resolution.

Similar to our the results in the Arctic Ocean, improving circulation with higher model resolution has also been shown to be the key driver for an improved representation of anthropogenic tracers in the Southern Ocean (Lachkar et al., 2007) or oxygen concentrations in the tropics (Duteil et al., 2014).

4.5 CMIP5 comparison

For wider perspective, we compared the forced NEMO-PISCES simulations to nine ocean biogeochemical models that were coupled within different earth system modeling frameworks as part of CMIP5 (Fig. 9). When the CMIP5 models are compared to the corrected data-based estimate of the ~~C_{ant}~~ C_{ant} inventory (Sect. 4.2), only the MIROC-ESM ~~and NorESM1-ME models with their inventories~~ with its inventory of 2.7 Pg C ~~and 2.4 Pg C fall within our simplistic revision of~~ fall within the data-based uncertainty estimate (~~2.2 to 3.0~~2.5 to 3.3 Pg C in 2005). Nearby ~~though is the~~ is the NorESM1-ME and HadGEM2-ES, which ~~falls~~ fall below the lower limit by ~~0.2~~0.1 and 0.5 Pg C, receptively. Further off are the MPI-ESM and GFDL-ESM models with their ~~C_{ant}~~ C_{ant} inventories in 2005 that are ~~0.6 to 1.2~~ 0.9 to 1.5 Pg C lower than the lower limit. The lowest estimates ~~though~~

are from both versions of the IPSL model whose inventories reach only ~~25~~20% of the lower limit of our revised data-based range. Adjusting the CMIP5-model Arctic inventories upward by ~0.4 Pg C to account for their late start date in 1850, as we did for our three simulations, would place ~~three~~ two of them (MIROC-ESM, and NorESM1-ME~~, and HadGEM2-ES~~) above the lower boundary of our revised data-based uncertainty estimate, and HadGEM2-ES just 0.1 Pg C below this lower boundary. For the cumulative air-sea flux between 1960 and 2012, for which there is no data-based constraint, all models fall between 0.3 and 1.2 Pg C. Lateral fluxes also vary between models, from an outflow of 0.3 Pg C in the IPSL-CM5A-LR model and an inflow of 1.1 Pg C in the MIROC-ESM model. Only the first three CMIP5 models mentioned above exhibit large net inflow of ~~C_{ant}~~ C_{ant} into the Arctic basin (between 0.7 and 1.1 Pg C from 1960–2012), a condition that appears necessary to allow a model to approach the estimated data-based inventory range. Indeed, the six other CMIP5 models have lower lateral fluxes (-0.5 to 0.5 Pg C) and simulate low ~~C_{ant}~~ C_{ant} storage in 2005.

What is perhaps most surprising are the large differences between our forced ORCA2 model and the IPSL-CM5A-LR and IPSL-CM5A-MR ESMs. All three of those models use ORCA2, although both ESMs rely on an earlier version with a different vertical resolution (31 instead of 46 vertical levels). That contrast in vertical resolution may explain part of the large differences in inventory (1.5 Pg C for our forced version vs. 0.3–0.6 Pg C for the two coupled versions) but the forcing and different model parameters could just as well be responsible. Thus lateral resolution is not the only factor when aiming to provide realistic simulations of ~~C_{ant}~~ C_{ant} storage and lateral transport in the Arctic. Sensitivity studies testing other potentially critical factors are clearly merited.

4.6 Effect on aragonite saturation state

Given that ~~C_{ant}~~ C_{ant} is affected by lateral model resolution, so must be ocean acidification. The aragonite saturation state (Ω_A) was computed for each resolution from the historical run's C_T, A_T, T, S, P_T, and Si_T, after correcting C_T and A_T for drift based on the control run. The higher concentrations of ~~C_{ant}~~ C_{ant} in the ORCA05 and ORCA025 simulations reduces Ω_A between 1960 and 2012 by more than twice as much as found with the ORCA2 model during the same period (Fig. 10). These differences translate into different rates of shoaling for the aragonite saturation horizon (ASH), i.e., the depth where $\Omega_A = 1$. During 1960–2012, the ASH shoals by ~50 m in ORCA2, while it shoals by ~150 m in ORCA05 and ~210 m in ORCA025. Thus model resolution also affects the time at which waters become undersaturated with respect to aragonite with higher resolution producing greater shoaling.

Although basin-wide mean surface Ω_A does not differ among resolutions, there are regional differences such as over the Siberian shelf (Fig. 11). While the minimum Ω_A in that region reaches 0.9 in ORCA2, it drops to ~~0.4~~ 0.3 in ORCA05 and 0.1 in ORCA025. That lower value in ORCA025 is more like that observed, e.g., down to 0.01 in the Laptev Sea (Semiletov et al., 2016). As these low extremes in Ω_A are extremely local, they cannot be expected to be captured in coarse-resolution models (ORCA2). Higher-resolution models are needed in the Arctic to assess local extremes not only in terms of ocean acidification but also other biogeochemical variables.

5 Conclusions

Global-ocean biogeochemical model simulations typically have coarse resolution and tend to underestimate the mass of ~~C_{ant}~~ C_{ant} stored in the Arctic Ocean. Our sensitivity tests suggest that more realistic results are offered by higher-resolution model configurations that begin to explicitly resolve ocean eddies. Our highest resolution model falls within the uncertainty range of Tanhua et al. (2009)'s data-based estimate for ~~C_{ant}~~ C_{ant} storage in the Arctic Ocean (2.5–3.3 Pg C in 2005). Yet that data-based range may need to be adjusted downward. Data-based ~~C_{ant}~~ C_{ant} concentrations below 2000 m remain at about 6 μmol kg^{-1}, while observed CFC-12 concentrations upon which they are based are close to negligible, being proportionally much smaller relative to near-surface concentrations. ~~Zeroing out the C_{ant}~~ A lower limit is estimated by zeroing out the C_{ant} concentrations below 2000 m in the GLODAPv2 climatology (Lauvset et al., 2016)~~reduces the~~. Thus, the lower limit of the data-based estimates for Arctic Ocean ~~C_{ant} storage~~ C_{ant} storage would be reduced by 10% to 2.2~~–3.0~~ Pg C in 2005. That ~~revised range~~ lower limit encompasses the adjusted simulated basin-wide inventories from the two higher resolutions, ORCA05 and ORCA025 (2.4 and 2.6 Pg C). ~~Details differ though~~At the same time, our highest resolution inventory is likely an underestimation as it was initialized in 1958 with ORCA05 results from 1765–1957. Details in model-data based comparison differ, e.g., with the ORCA025 results underestimating ~~C_{ant}~~ C_{ant} data-based estimates at around 400 m and overestimating them at around ~~800~~1300 m. That deeper model overestimate appears due to excessive penetration of ~~C_{ant}~~C_{ant}-rich Atlantic water. The shallower model underestimate may be due to inadequate representation of ventilation of intermediate waters via down-slope flows that are driven by brine formation over the Arctic's enormous continental shelf, a transport process that is notoriously difficult to represent in z-coordinate models, especially at lower resolution.

Data-based estimates of ~~C_{ant}~~ C_{ant} in the Arctic Ocean might be improved by testing the TTD method in the model, using the same approach but with modeled CFC-12 and temperature and then comparing the resulting calculated ~~C_{ant}~~ C_{ant} to the directly simulated ~~C_{ant}~~C_{ant}. With a series of those calculations, the parameters of the TTD approach (Δ/Γ) could be varied and the best ratio selected for the closest match between calculated and simulated ~~C_{ant}~~C_{ant}. Then that chosen ratio could be applied to the observed CFC-12 rather than using the default ratio of $\Delta/\Gamma = 1$. We leave this effort for future work.

Our forced ocean simulations suggest that Arctic Ocean storage of ~~C_{ant}~~ C_{ant} is driven mostly by net lateral inflow, the total input of which is about three times that from the air-sea flux. That 3:1 ratio varies little with resolution because the lateral flux and the air-sea flux both increase as resolution is refined. Lateral fluxes in the CMIP5 models are generally less dominant but are also highly inconsistent both in magnitude and in the lateral:air-sea flux ratio. Some CMIP5 models even simulate net lateral outflow of ~~C_{ant}~~ C_{ant} and unrealistically low ~~C_{ant}~~ C_{ant} inventories. The only CMIP5 models that succeed in reaching the lower limit of the data-based ~~C_{ant}~~ C_{ant} inventory range are those that have a large net lateral input. The causes of the CMIP5 model differences remain unclear as is often the case when comparing models having many differences. We expect that most of the CMIP5 models have not been evaluated in terms of their ability to simulate realistic lateral water transport at the boundaries of the Arctic Ocean, which is fundamental to simulating realistic ~~C_{ant}~~ C_{ant} but may be problematic given their coarse resolution. The next phase of CMIP (CMIP6) plans to include CFC-12 and related transient transient tracers, which will help weigh simulated results for ~~C_{ant}~~C_{ant}.

As the mass of simulated anthropogenic carbon in the Arctic Ocean increases with resolution, so does the simulated acidification. For instance, during 1960–2012, the average ASH in the Arctic shoals four times faster in ORCA025 than in ORCA2. Higher resolution is also needed to capture local extremes. Although higher horizontal resolution appears necessary to improve fine-scale future projections of Arctic Ocean acidification, the computational costs of centennial-scale, high-resolution, biogeochemical ocean simulations remain prohibitive. More practical in the short term would be to assess effects from less-costly model improvements, including heightened vertical resolution, subgrid-scale parameterizations, and adjustments to model parameters for viscosity and slip conditions. For such regional studies, nested models would offer the advantage of focused higher resolution while still avoiding adverse effects from imposed lateral boundary conditions.

Code availability. The code for the NEMO ocean model version 3.2 is available under CeCILL license at http://www.nemo-ocean.eu.

Competing interests. The authors declare that there are not competing interests.

Acknowledgements. We thank J. Simeon for the first implementation of the ORCA05 and ORCA025 versions of the model. The research leading to these results was supported through the EU H2020 project C-CASCADES (Marie Sklodowska-Curie grant 643052). LB and JCO acknowledge support of the EU H2020 CRESCENDO project (grant 641816) and the ANR SOBUMS project (ANR-16-CE01-0014). LB acknowledges support from the MTES Acidoscope project. Simulations were made using HPC resources from the French GENCI-IDRIS program (grant x2015010040). Model output was stored and analyzed on the Ciclad platform at the IPSL.

References

Aksenov, Y., Karcher, M., Proshutinsky, A., Gerdes, R., De Cuevas, B., Golubeva, E., Kauker, F., Nguyen, A. T., Platov, G. A., Wadley, M., et al.: Arctic pathways of Pacific Water: Arctic Ocean model intercomparison experiments, J. Geophys. Res. Oceans, 121, 27–59, doi:10.1002/2015JC011299, 2016.

Anderson, L., Tanhua, T., Jones, E., and Karlqvist, A.: Hydrographic, chemical and carbon dioxide data from R/V Oden cruise 77DN20050819, August 19 - September 25, 2005, doi:10.3334/CDIAC/otg.CLIVAR_77DN20050819, 2011.

Aumont, O. and Bopp, L.: Globalizing results from ocean in situ iron fertilization studies, Global Biogeochem. Cycles, 20, doi:10.1029/2005GB002591, 2006.

Barnier, B., Madec, G., Penduff, T., Molines, J.-M., Treguier, A.-M., Le Sommer, J., Beckmann, A., Biastoch, A., Böning, C., Dengg, J., et al.: Impact of partial steps and momentum advection schemes in a global ocean circulation model at eddy-permitting resolution, Ocean Dyn., 56, 543–567, doi:10.1007/s10236-006-0082-1, 2006.

Bates, N. and Mathis, J.: The Arctic Ocean marine carbon cycle: evaluation of air-sea CO 2 exchanges, ocean acidification impacts and potential feedbacks, Biogeosciences, 6, 2433–2459, doi:10.5194/bg-6-2433-2009, 2009.

Bekryaev, R. V., Polyakov, I. V., and Alexeev, V. A.: Role of polar amplification in long-term surface air temperature variations and modern Arctic warming, J. Clim., 23, 3888–3906, doi:10.1175/2010JCLI3297.1, 2010.

Bourgeois, T., Orr, J. C., Resplandy, L., Terhaar, J., Ethé, C., Gehlen, M., and Bopp, L.: Coastal-ocean uptake of anthropogenic carbon, Biogeosciences, 13, 4167–4185, doi:10.5194/bg-13-4167-2016, 2016.

Brewer, P. G.: Direct observation of the oceanic CO2 increase, Geophys. Res. Lett., 5, 997–1000, doi:10.1029/GL005i012p00997, 1978.

Brodeau, L., Barnier, B., Treguier, A.-M., Penduff, T., and Gulev, S.: An ERA40-based atmospheric forcing for global ocean circulation models, Ocean Model., 31, 88–104, doi:10.1016/j.ocemod.2009.10.005, 2010.

Broecker, W., Takahashi, T., and Peng, T.: Reconstruction of past atmospheric CO_2 contents from the chemistry of the contemporary ocean: an evaluation, Tech. Rep. DOE/OR-857, US Department of Energy, Washington DC, 1985.

Bronselaer, B., Winton, M., Russell, J., Sabine, C. L., and Khatiwala, S.: Agreement of CMIP5 Simulated and Observed Ocean Anthropogenic CO2 Uptake, Geophys. Res. Lett., 44, 12,298–12,305, doi:10.1002/2017GL074435, 2017.

Bullister, J. L.: Atmospheric Histories (1765-2015) for CFC-11, CFC-12, CFC-113, CCl4, SF6 and N2O, Carbon Dioxide Information Analysis Center, Oak Ridge National Laboratory, US Department of Energy, Oak Ridge, Tennessee, 2015.

Chen, G.-T. and Millero, F. J.: Gradual increase of oceanic CO2, Nature, 277, 205–206, doi:10.1038/277205a0, 1979.

Conkright, M. E., Garcia, H. E., O'Brien, T. D., Locarnini, R. A., Boyer, T. P., Stephens, C., and Antonov, J. I.: World Ocean Atlas 2001, NOAA Atlas NESDIS 52, NOAA, Silver Spring, Md, p. 392pp., 2002.

Curry, B., Lee, C., Petrie, B., Moritz, R., and Kwok, R.: Multiyear volume, liquid freshwater, and sea ice transports through Davis Strait, 2004–10, J. Phys. Oceanogr., 44, 1244–1266, doi:10.1175/JPO-D-13-0177.1, 2014.

Dickson, A. G., Sabine, C. L., and Christian, J. R.: Guide to best practices for ocean CO_2 measurements, Tech. rep., PICES Special Publication 3, 191 pp., 2007.

Dutay, J.-C., Bullister, J., Doney, S., Orr, J., Najjar, R., Caldeira, K., Campin, J.-M., Drange, H., Follows, M., Gao, Y., Gruber, N., Hecht, M., Ishida, A., Joos, F., Lindsay, K., Madec, G., Maier-Reimer, E., Marshall, J., Matear, R., Monfray, P., Mouchet, A., Plattner, G.-K., Sarmiento, J., Schlitzer, R., Slater, R., Totterdell, I., Weirig, M.-F., Yamanaka, Y., and Yool, A.: Evaluation of ocean model ventilation

with CFC-11: comparison of 13 global ocean models, Ocean Model., 4, 89 – 120, doi:https://doi.org/10.1016/S1463-5003(01)00013-0, 2002.

Duteil, O., Schwarzkopf, F. U., Böning, C. W., and Oschlies, A.: Major role of the equatorial current system in setting oxygen levels in the eastern tropical Atlantic Ocean: A high-resolution model study, Geophysical Research Letters, 41, 2033–2040, doi:10.1002/2013GL058888, 2014.

Gattuso, J.-P. and Hansson, L.: Ocean acidification, Oxford University Press, Oxford, 2011.

Gent, P. R. and Mcwilliams, J. C.: Isopycnal mixing in ocean circulation models, J. Phys. Oceanogr., 20, 150–155, doi:10.1175/1520-0485(1990)020<0150:IMIOCM>2.0.CO;2, 1990.

Gruber, N., Sarmiento, J. L., and Stocker, T. F.: An improved method for detecting anthropogenic CO2 in the oceans, Global Biogeochem. Cycles, 10, 809–837, doi:10.1029/96GB01608, 1996.

Hall, T. M., Haine, T. W., and Waugh, D. W.: Inferring the concentration of anthropogenic carbon in the ocean from tracers, Global Biogeochem. Cycles, 16, doi:10.1029/2001GB001835, 2002.

Jakobsson, M.: Hypsometry and volume of the Arctic Ocean and its constituent seas, Geochem. Geophys., 3, 1–18, doi:10.1029/2001GC000302, 2002.

Jakobsson, M., Cherkis, N., Woodward, J., Macnab, R., and Coakley, B.: New grid of Arctic bathymetry aids scientists and mapmakers, Eos, Trans. Amer. Geophys. Union, 81, 89–96, doi:10.1029/00EO00059, 2000.

Jeansson, E., Olsen, A., Eldevik, T., Skjelvan, I., Omar, A. M., Lauvset, S. K., Nilsen, J. E. O., Bellerby, R. G. J., Johannessen, T., and Falck, E.: The Nordic Seas carbon budget: Sources, sinks, and uncertainties, Global Biogeochem. Cycles, 25, doi:10.1029/2010GB003961, 2011.

Jones, E., Rudels, B., and Anderson, L.: Deep waters of the Arctic Ocean: origins and circulation, Deep Sea Res. Part I Oceanogr. Res. Pap., 42, 737–760, doi:10.1016/0967-0637(95)00013-V, 1995.

Jones, P., Azetsu-Scott, K., Aagaard, K., Carmack, E., and Swift, J.: L.S. St. Laurent 18SN19940724, AOS94 cruise data from the 1994 cruises, CARINA Data Set, doi:10.3334/CDIAC/otg.CARINA_18SN19940724, 2007.

Key, R. M., Kozyr, A., Sabine, C. L., Lee, K., Wanninkhof, R., Bullister, J. L., Feely, R. A., Millero, F. J., Mordy, C., and Peng, T.-H.: A global ocean carbon climatology: Results from Global Data Analysis Project (GLODAP), Global Biogeochem. Cycles, 18, doi:10.1029/2004GB002247, 2004.

Khatiwala, S., Primeau, F., and Hall, T.: Reconstruction of the history of anthropogenic CO2 concentrations in the ocean, Nature, 462, 346, doi:10.1038/nature08526, 2009.

Khatiwala, S., Tanhua, T., Fletcher, S. M., Gerber, M., Doney, S., Graven, H., Gruber, N., McKinley, G., Murata, A., Ríos, A., et al.: Global ocean storage of anthropogenic carbon, Biogeosciences, 10, 2169–2191, doi:10.5194/bg-10-2169-2013, 2013.

Lachkar, Z., Orr, J. C., Dutay, J.-C., and Delecluse, P.: Effects of mesoscale eddies on global ocean distributions of CFC-11, CO₂, and ?¹⁴C, Ocean Science, 3, 461–482, 2007.

Lauvset, S. K., Key, R. M., and Perez, F. F.: A new global interior ocean mapped climatology: the $1^\circ \times 1^\circ$ GLODAP version 2, Earth Syst. Sci. Data, 8, 325, doi:10.5194/essd-8-325-2016, 2016.

Le Quéré, C., Moriarty, R., Andrew, R., Peters, G., Ciais, P., Friedlingstein, P., Jones, S., Sitch, S., Tans, P., Arneth, A., et al.: Global carbon budget 2014, Earth Syst. Sci. Data, 7, 47–85, doi:10.5194/essd-7-47-2015, 2015.

Ludwig, W., Amiotte-Suchet, P., Munhoven, G., and Probst, J.-L.: Atmospheric CO_2 consumption by continental erosion: present-day controls and implications for the last glacial maximum, Glob. Planet. Change, 16, 107–120, doi:10.1016/S0921-8181(98)00016-2, 1998.

Luo, Y., Boudreau, B. P., and Mucci, A.: Disparate acidification and calcium carbonate desaturation of deep and shallow waters of the Arctic Ocean, Nat. Commun., 7, 12 821, doi:10.1038/ncomms12821, 2016.

Lythe, M. B. and Vaughan, D. G.: BEDMAP: A new ice thickness and subglacial topographic model of Antarctica, J. Geophys. Res. Solid Earth, 106, 11 335–11 351, doi:10.1029/2000JB900449, 2001.

Madec, G.: NEMO ocean engine, Note du Pôle de modélisation, Institut Pierre-Simon Laplace (IPSL), France, No 27, ISSN No 1288-1619, 2008.

Madec, G., Delecluse, P., Imbard, M., and Levy, C.: Ocean general circulation model reference manual, Note du Pôle de modélisation, Institut Pierre-Simon Laplace (IPSL), France, 1998.

McClelland, J. W., Déry, S. J., Peterson, B. J., Holmes, R. M., and Wood, E. F.: A pan-arctic evaluation of changes in river discharge during the latter half of the 20th century, Geophys. Res. Lett., 33, doi:10.1029/2006GL025753, 2006.

Meinshausen, M., Vogel, E., Nauels, A., Lorbacher, K., Meinshausen, N., Etheridge, D. M., Fraser, P. J., Montzka, S. A., Rayner, P. J., Trudinger, C. M., Krummel, P. B., Beyerle, U., Canadell, J. G., Daniel, J. S., Enting, I. G., Law, R. M., Lunder, C. R., O'Doherty, S., Prinn, R. G., Reimann, S., Rubino, M., Velders, G. J. M., Vollmer, M. K., Wang, R. H. J., and Weiss, R.: Historical greenhouse gas concentrations for climate modelling (CMIP6), Geosci. Model Dev., 10, 2057–2116, doi:10.5194/gmd-10-2057-2017, 2017.

Meybeck, M.: Carbon, nitrogen, and phosphorus transport by world rivers, Am. J. Sci, 282, 401–450, doi:10.2475/ajs.282.4.401, 1982.

Moore, J. K., Doney, S. C., and Lindsay, K.: Upper ocean ecosystem dynamics and iron cycling in a global three-dimensional model, Global Biogeoch. Cycles, 18, doi:10.1029/2004GB002220, 2004.

Olsen, A., Anderson, L. G., and Heinze, C.: Arctic Carbon Cycle: Patterns, Impacts and Possible Changes, in: The New Arctic, edited by Evengård, B., Nymand Larsen, J., and Paasche, Ø., pp. 95–115, Springer International Publishing, Cham, doi:10.1007/978-3-319-17602-4_8, 2015.

Orr, J. C., Monfray, P., Maier-Reimer, E., Mikolajewicz, U., Palmer, J., Taylor, N. K., Toggweiler, J. R., Sarmiento, J. L., Quéré, C. L., Gruber, N., Sabine, C. L., Key, R. M., and Boutin, J.: Estimates of anthropogenic carbon uptake from four three-dimensionsal global ocean models, Global Biogeochem. Cycles, 15, 43–60, doi:10.1029/2000GB001273, 2001.

Orr, J. C., Najjar, R. G., Aumont, O., Bopp, L., Bullister, J. L., Danabasoglu, G., Doney, S. C., Dunne, J. P., Dutay, J.-C., Graven, H., et al.: Biogeochemical protocols and diagnostics for the CMIP6 Ocean Model Intercomparison Project (OMIP), Geosci. Model Dev., 10, 2169, doi:10.5194/gmd-10-2169-2017, 2017.

Popova, E., Yool, A., Aksenov, Y., and Coward, A.: Role of advection in Arctic Ocean lower trophic dynamics: A modeling perspective, J. Geophys. Res.: Oceans, 118, 1571–1586, doi:10.1002/jgrc.20126, 2013.

Proshutinsky, A., Steele, M., and Timmermans, M.-L.: Forum for Arctic Modeling and Observational Synthesis (FAMOS): Past, current, and future activities, J. Geophys. Res.: Oceans, 121, 3803–3819, doi:10.1002/2016JC011898, 2016.

Rudels, B., Jones, E. P., Anderson, L. G., and Kattner, G.: On the Intermediate Depth Waters of the Arctic Ocean, in: The Polar Oceans and Their Role in Shaping the Global Environment, edited by Johannessen, O. M., Muench, R. D., and Overland, J. E., pp. 33–46, American Geophysical Union, Washington DC, doi:10.1029/GM085p0033, 1994.

Rudels, B., Marnela, M., and Eriksson, P.: Constraints on estimating mass, heat and freshwater transports in the Arctic Ocean: An exercise, in: Arctic–Subarctic Ocean Fluxes, pp. 315–341, Springer, Dordrecht, Netherlands, 2008.

Sabine, C. L., Feely, R. A., Gruber, N., Key, R. M., Lee, K., Bullister, J. L., Wanninkhof, R., Wong, C., Wallace, D. W., Tilbrook, B., et al.: The oceanic sink for anthropogenic CO2, Science, 305, 367–371, doi:10.1126/science.1097403, 2004.

Sarmiento, J. L., Orr, J. C., and Siegenthaler, U.: A perturbation simulation of CO2 uptake in an ocean general circulation model, J. Geophys. Res.: Oceans, 97, 3621–3645, doi:10.1029/91JC02849, 1992.

Schauer, U., Beszczynska-Möller, A., Walczowski, W., Fahrbach, E., Piechura, J., and Hansen, E.: Variation of measured heat flow through the Fram Strait between 1997 and 2006, in: Arctic–Subarctic Ocean Fluxes, pp. 65–85, Springer, Dordrecht, Netherlands, 2008.

Schlosser, P., Kromer, B., Östlund, G., Ekwurzel, B., Bönisch, G., Loosli, H. H., and Purtschert, R.: On the 14C and 39Ar Distribution in the Central Arctic Ocean: Implications for Deep Water Formation, Radiocarbon, 36, 327—343, doi:10.1017/S003382220001451X, 1994.

Semiletov, I., Pipko, I., Gustafsson, Ö., Anderson, L. G., Sergienko, V., Pugach, S., Dudarev, O., Charkin, A., Gukov, A., Bröder, L., et al.: Acidification of East Siberian Arctic Shelf waters through addition of freshwater and terrestrial carbon, Nat. Geosci., 9, 361–365, doi:10.1038/ngeo2695, 2016.

Skagseth, Ø., Furevik, T., Ingvaldsen, R., Loeng, H., Mork, K. A., Orvik, K. A., and Ozhigin, V.: Volume and heat transports to the Arctic Ocean via the Norwegian and Barents Seas, in: Arctic–Subarctic Ocean Fluxes, pp. 45–64, Springer, Dordrecht, Netherlands, 2008.

Smedsrud, L. H., Ingvaldsen, R., Nilsen, J. E. Ø., and Skagseth, Ø.: Heat in the Barents Sea: transport, storage, and surface fluxes, Ocean Sci., 6, 219–234, doi:10.5194/os-6-219-2010, 2010.

Smith, W. H. and Sandwell, D. T.: Global sea floor topography from satellite altimetry and ship depth soundings, Science, 277, 1956–1962, doi:10.1126/science.277.5334.1956, 1997.

Steinacher, M., Joos, F., Frolicher, T. L., Plattner, G.-K., and Doney, S. C.: Imminent ocean acidification in the Arctic projected with the NCAR global coupled carbon cycle-climate model, Biogeosciences, 6, 515–533, doi:10.5194/bg-6-515-2009, 2009.

Straneo, F. and Saucier, F.: The outflow from Hudson Strait and its contribution to the Labrador Current, Deep Sea Res. Part I Oceanogr. Res. Pap., 55, 926–946, doi:10.1016/j.dsr.2008.03.012, 2008.

Stöven, T., Tanhua, T., Hoppema, M., and Wilken-Jon, v. A.: Transient tracer distributions in the Fram Strait in 2012 and inferred anthropogenic carbon content and transport, Ocean Sci., 12, 319–333, doi:10.5194/os-12-319-2016, 2016.

Takahashi, T., Broecker, W. S., and Langer, S.: Redfield ratio based on chemical data from isopycnal surfaces, J. Geophys. Res.: Oceans, 90, 6907–6924, doi:10.1029/JC090iC04p06907, 1985.

Tanhua, T., Jones, E. P., Jeansson, E., Jutterström, S., Smethie, W. M., Wallace, D. W., and Anderson, L. G.: Ventilation of the Arctic Ocean: Mean ages and inventories of anthropogenic CO2 and CFC-11, J. Geophys. Res.: Oceans, 114, doi:10.1029/2008JC004868, 2009.

Taylor, K. E., Stouffer, R. J., and Meehl, G. A.: An Overview of CMIP5 and the Experiment Design, Bull. Am. Meteorol. Soc., 93, 485–498, doi:10.1175/bams-d-11-00094.1, https://doi.org/10.1175/bams-d-11-00094.1, 2012.

Tegen, I. and Fung, I.: Contribution to the atmospheric mineral aerosol load from land surface modification, J. Geophys. Res.: Atmos., 100, 18 707–18 726, doi:10.1029/95JD02051, 1995.

Vancoppenolle, M., Fichefet, T., Goosse, H., Bouillon, S., Madec, G., and Maqueda, M. A. M.: Simulating the mass balance and salinity of Arctic and Antarctic sea ice. 1. Model description and validation, Ocean Model., 27, 33 – 53, doi:10.1016/j.ocemod.2008.10.005, 2009.

Walsh, J. E., Chapman, W. L., and Fetterer, F.: Gridded Monthly Sea Ice Extent and Concentration, 1850 Onward, Version 1. [1979 to 2010], doi:http://dx.doi.org/10.7265/N5833PZ5, Boulder, Colorado USA. NSIDC: National Snow and Ice Data Center, 2015.

Wanninkhof, R.: Relationship between wind speed and gas exchange over the ocean, Journal of Geophysical Research: Oceans, 97, 7373–7382, doi:10.1029/92JC00188, 1992.

Warner, M. and Weiss, R.: Solubilities of chlorofluorocarbons 11 and 12 in water and seawater, Deep Sea Res. Part A Oceanogr. Res. Pap., 32, 1485 – 1497, doi:https://doi.org/10.1016/0198-0149(85)90099-8, http://www.sciencedirect.com/science/article/pii/0198014985900998, 1985.

Waugh, D., Hall, T., McNeil, B., Key, R., and Matear, R.: Anthropogenic CO2 in the oceans estimated using transit time distributions, Tellus B, 58, 376–389, doi:10.1111/j.1600-0889.2006.00222.x, 2006.

Waugh, D. W., Haine, T. W., and Hall, T. M.: Transport times and anthropogenic carbon in the subpolar North Atlantic Ocean, Deep Sea Res. Part I Oceanogr. Res. Pap., 51, 1475–1491, doi:10.1016/j.dsr.2004.06.011, 2004.

Willey, D. A., Fine, R. A., Sonnerup, R. E., Bullister, J. L., Smethie Jr., W. M., and Warner, M. J.: Global oceanic chlorofluorocarbon inventory, Geophys. Res. Lett., 31, L01303, doi:10.1029/2003GL018816, 2004.

Woodgate, R.: Arctic Ocean circulation: Going around at the top of the world, Nat. Edu. Knowl., 4, 8, 2013.

Woodgate, R. A., Weingartner, T., and Lindsay, R.: The 2007 Bering Strait oceanic heat flux and anomalous Arctic sea-ice retreat, Geophys. Res. Lett., 37, doi:10.1029/2009GL041621, l01602, 2010.

Yang, D.: An improved precipitation climatology for the Arctic Ocean, Geophys. Res. Lett., 26, 1625–1628, doi:10.1029/1999GL900311, 1999.

Table 1. Grid size in the Arctic Ocean and volumes by basin as a function of model resolution.

Configuration	Horizontal grid (km)			Volume (10^6 km^3)				
					Basins			
	Mean	Min	Max	Arctic	Nansen	Amundsen	Makarov	Canada
ORCA2	120.8	63.3	180.5	14.3	2.8	3.2	2.2	4.7
ORCA05	29.0	9.4	41.3	13.3	2.6	2.7	1.9	4.9
ORCA025	14.4	3.2	20.5	13.3	2.3	2.9	1.8	5.0

Table 2. Selected physical coefficients and parameters for ORCA2, ORCA05, and ORCA025.

Configuration	Lateral diffusivity	Lateral viscosity	Eddy parameterization
ORCA2[a]	2000 $m^2\ s^{-1}$	4×10^4 $\mathrm{m}^2\ \mathrm{s}^{-1}$ [a] [b]	2000 $\mathrm{m}^2\ \mathrm{s}^{-1}$
ORCA05	600 $m^2\ s^{-1}$	-4 $\times 10^{11}$ $\mathrm{m}^2\ \mathrm{s}^{-1}$	1000 $\mathrm{m}^2\ \mathrm{s}^{-1}$
ORCA025	300 $m^2\ s^{-1}$	-1.5 $\times 10^{11}$ $\mathrm{m}^2\ \mathrm{s}^{-1}$	none

[a] Lateral diffusivity and viscosity coefficients decrease towards the poles proportional to the grid size.

[b] reduced to 2100 $\mathrm{m}^2\ \mathrm{s}^{-1}$ in the tropics (except along Western boundaries)

Table 3. Fitted parameters for the perturbation ~~approach for the traces starting in 1765 (~~simulations P1765 ~~)~~ and ~~in 1870 (~~P1870~~)~~.

Parameter	P1765	P1870
~~a_0~~ a_0	1.7481	1.8302
~~a_1~~ a_1	-3.2813 $\times 10^{-2}$	-3.4631 $\times 10^{-2}$
~~a_2~~ a_2	4.1855 $\times 10^{-4}$	4.3614 $\times 10^{-4}$
~~b_0~~ b_0	3.9615 $\times 10^{-3}$	4.0105 $\times 10^{-3}$
~~b_1~~ b_1	-7.3733 $\times 10^{-5}$	-7.3386 $\times 10^{-5}$
~~b_2~~ b_2	5.4759 $\times 10^{-5}$	5.1199 $\times 10^{-5}$

~~Grid size in the Arctic Ocean and volumes by basin as a function of model resolution. Configuration Mean Min Max Arctic Nansen Amundsen Makarov Canada ORCA2 120.8 63.3 180.5 14.3 2.8 3.2 2.2 4.7ORCA05 29.0 9.4 41.3 13.3 2.6 2.7 1.9 4.9ORCA025 14.4 3.2 20.5 13.3 2.3 2.9 1.8 5.0~~

Table 4. Lateral transport of water and ~~C_{ant}~~ C_{ant} across Arctic Ocean boundaries. Simulated values are calculated for the same time period as observations.

	Model configuration			Observations	Year	Sources
	ORCA2	ORCA05	ORCA025			
Lateral water transport (Sv)						
Fram Strait	-1.76	-1.75	-1.80	-2.0 ± 2.7	1997–2006	Schauer et al. (2008)
	-1.76	-1.42	-1.46	-1.7	1980–2005	Rudels et al. (2008)
Barents Sea	1.20	2.50	2.77	2.0	2003–2005	Skagseth et al. (2008)
	1.04	2.42	2.78	2.0	1997–2007	Smedsrud et al. (2010)
Bering Strait	1.02	1.29	1.49	0.8 ± 0.2	1991–2007	Woodgate et al. (2010)
CAA	-0.29	-2.00	-2.59	-2.7 ± 0.2	2004–2013	Curry et al. (2014)
~~Total transport~~ Sum	-0.12	-0.16	-0.18			

	Model configuration			Observations	Year	Sources
	ORCA2	ORCA05	ORCA025	~~P1765 P1870~~		
Lateral ~~C_{ant}~~ C_{ant} fluxes ($Tg\ C\ yr^{-1}$)						
Fram Strait	~~-14~~ -17	~~-10~~ -12	~~-6~~ -8	~~-12 -10~~ -1 ± 17	2002	Jeansson et al. (2011)
	~~-14~~ -17	~~-5~~ -7	~~7~~ 5	~~-6 -4~~ -12	2012	Stöven et al. (2016)
Barents Sea	~~14~~ 16	~~38~~ 43	~~44~~ 50	~~41 36~~ 41 ± 8	2002	Jeansson et al. (2011)
Bering Strait	~~16~~ 18	~~20 24~~ 22	~~20~~ 27	18	$2000 - 2010^a$	Olsen et al. (2015)
CAA	~~-4~~ -5	~~-25~~ -28	~~-31~~ -36	~~-26 -23~~ -29	$2000 - 2010^a$	Olsen et al. (2015)
~~Summed lateral flux~~ Sum	~~17~~ 18	~~28~~ 29	~~37~~38	~~30~~ 29	~~29~~ $2000 - 2010^a$	Olsen et al. (2015)

[a] Year or period impossible to identify exactly as C_{ant} and velocity measurements are not from the same year

Table 5. Total inventory, its change during 1960–2012, cumulative air-sea flux, and lateral flux of ~~C_{ant}~~ C_{ant} in Pg C

	Model configuration		
	ORCA2	ORCA05	ORCA025 ~~P1765 P1870~~
~~C_{ant}~~ C_{ant} **inventory**[a]			
~~C_{ant}~~ C_{ant} in 2002[b]	~~1.47 (1.88~~1.90 (1.47)	~~1.81 (~~2.25 (1.81)	~~2.06 (2.47) 2.04 1.63~~ 2.49 (2.06)
~~C_{ant}~~ C_{ant} in 2005[c]	~~1.56 (1.97~~1.99 (1.56)	~~1.96 (~~2.37 (1.96)	~~2.21 (2.62) 2.15 1.74~~ 2.64 (2.21)
Inventory change (1960-2012)			
Total Arctic	~~1.04~~ 1.08	~~1.50~~ 1.55	~~1.91 1.39 1.34~~ 1.98
Nansen Basin	0.14	0.33	~~0.29~~ 0.30 ~~0.30~~
Amundsen Basin	0.13	~~0.27~~ 0.28	~~0.33 0.25 0.24~~ 0.34
Makarov Basin	~~0.14~~ 0.15	~~0.20~~ 0.21	~~0.32 0.19 0.18~~ 0.33
Canada Basin	~~0.29 0.34 0.57~~ 0.31	~~0.29~~ 0.36	0.61
Cumulative fluxes (1960-2012)			
Air-Sea flux	0.29	~~0.42~~ 0.43	~~0.47 0.23 0.22~~ 0.48
Lateral flux of ~~C_{ant}~~ C_{ant}[d]	~~0.75~~ 0.79	~~1.08~~ 1.13	~~1.45 1.17 1.12~~ 1.50
Fram Strait	~~-0.59~~ -0.74	~~-0.29~~ -0.40	~~0.04 -0.36 -0.25~~ -0.06
Barents Sea	~~0.68~~ 0.79	~~1.51~~ 1.75	~~1.70 1.68 1.44~~1.98
Bering Strait	~~0.64~~ 0.74	~~0.77~~ 0.89	~~0.89 0.77~~1.03
CAA	~~-0.18~~ -0.22	~~-0.99~~ -1.20	~~-1.25 -1.13 -0.92~~-1.50
Summed lateral flux	~~0.55~~ 0.57	~~1.00~~ 1.05	~~1.39 1.09 1.04~~ 1.45

[a] Numbers in brackets show the uncorrected value (starting date 1870)

[b] Data-based inventory in 2002: 2.95 Pg C (GLODAPv2)

[c] Data-based inventory in 2005: 3.03 Pg C (2.5-3.3) (Tanhua et al., 2009)

[d] Computed as inventory change minus cumulative air-sea flux

Table 6. CFC-12 inventories [μmol m^{-1}] integrated over depth and distance along the AOS94 and Beringia 2005 expedition compared to results from ORCA2, ORCA05, and ORCA025 along the same sections.

	AOS94	Beringia 2005
Observation	5.5	9.4
ORCA2	4.8	7.7
ORCA05	3.5	5.8
ORCA025	2.9	3.7

~~Arctic Ocean C_{ant} inventory for the three biogeochemical simulation resolutions corrected for the late starting date. The intermediate-resolution model (ORCA05 - red dashed) was integrated from 1870 to 2012. The high-resolution model (ORCA025 - blue dash-dot) and the low-resolution model (ORCA2 - dotted green) were initialized with the ORCA05 output at the end of 1957 and integrated from 1958 to 2012. The discontinuity for ORCA2 in 1958 is due to its larger total volume of water when integrated across the Arctic domain (Table 1).~~

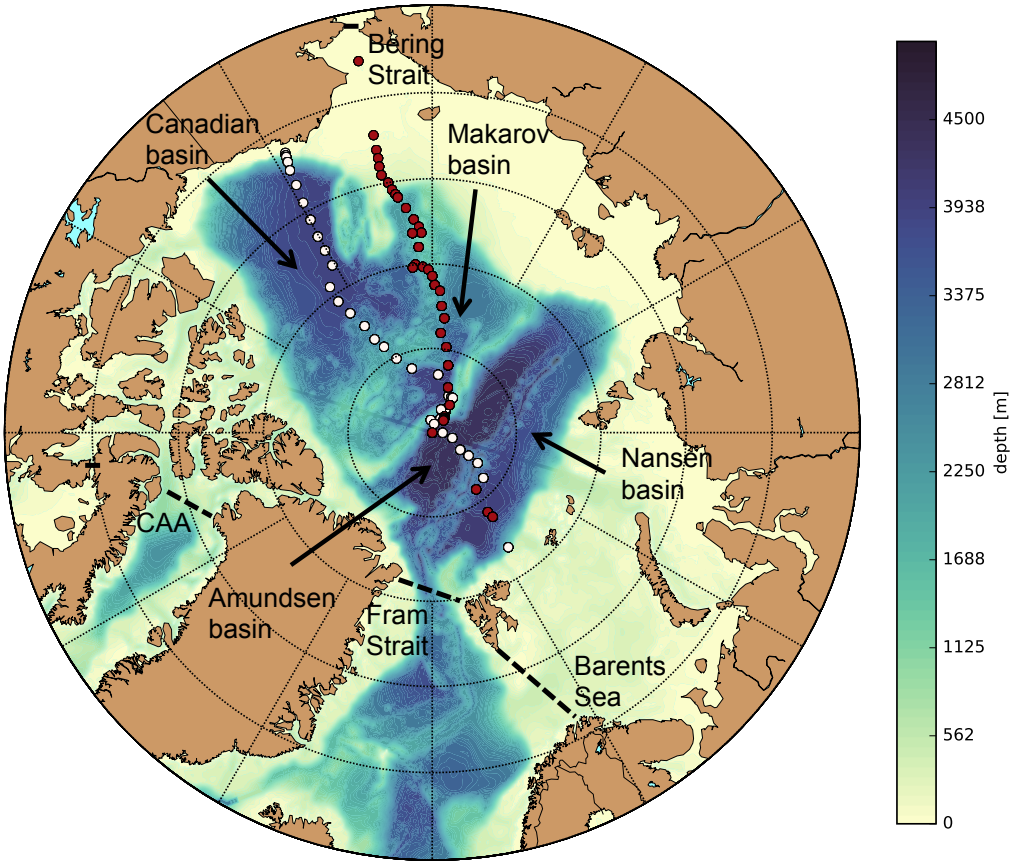

Figure 1. CFC-12 stations occupied during the AOS94 (red) and Beringia 2005 expedition (white). The filled-color scheme indicates the bathymetry of the Arctic Ocean, while the four dashed lines show the boundaries used in this study.

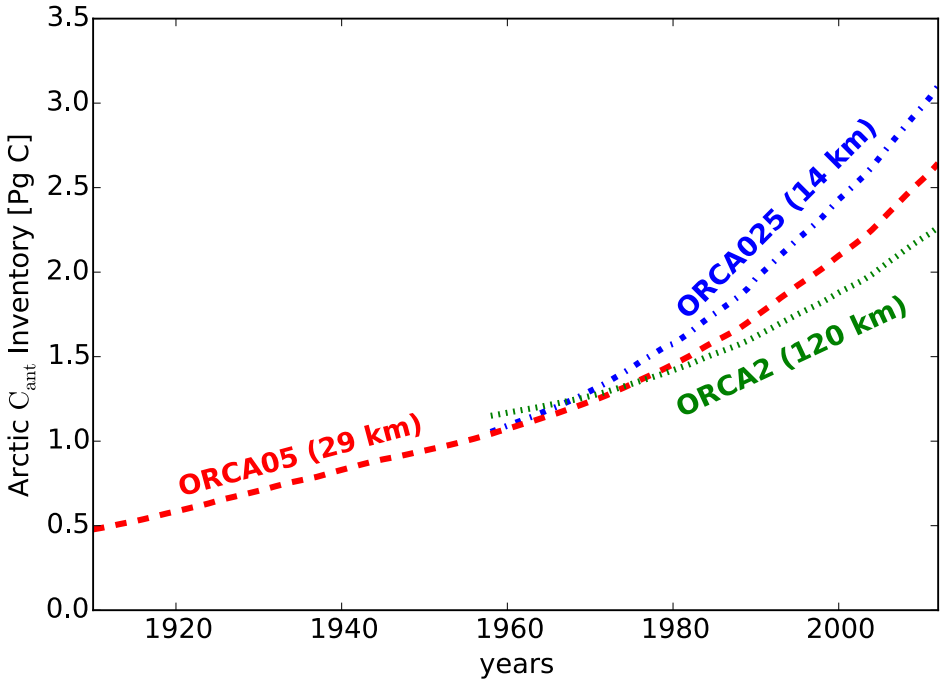

Figure 2. Arctic Ocean C_{ant} inventory for the three biogeochemical simulation resolutions corrected for the late starting date. The intermediate-resolution model (ORCA05 - red dashed) was integrated from 1870 to 2012. The high-resolution model (ORCA025 - blue dash-dot) and the low-resolution model (ORCA2 - dotted green) were initialized with the ORCA05 output at the end of 1957 and integrated from 1958 to 2012. The discontinuity for ORCA2 in 1958 is due to its larger total volume of water when integrated across the Arctic domain (Table 1).

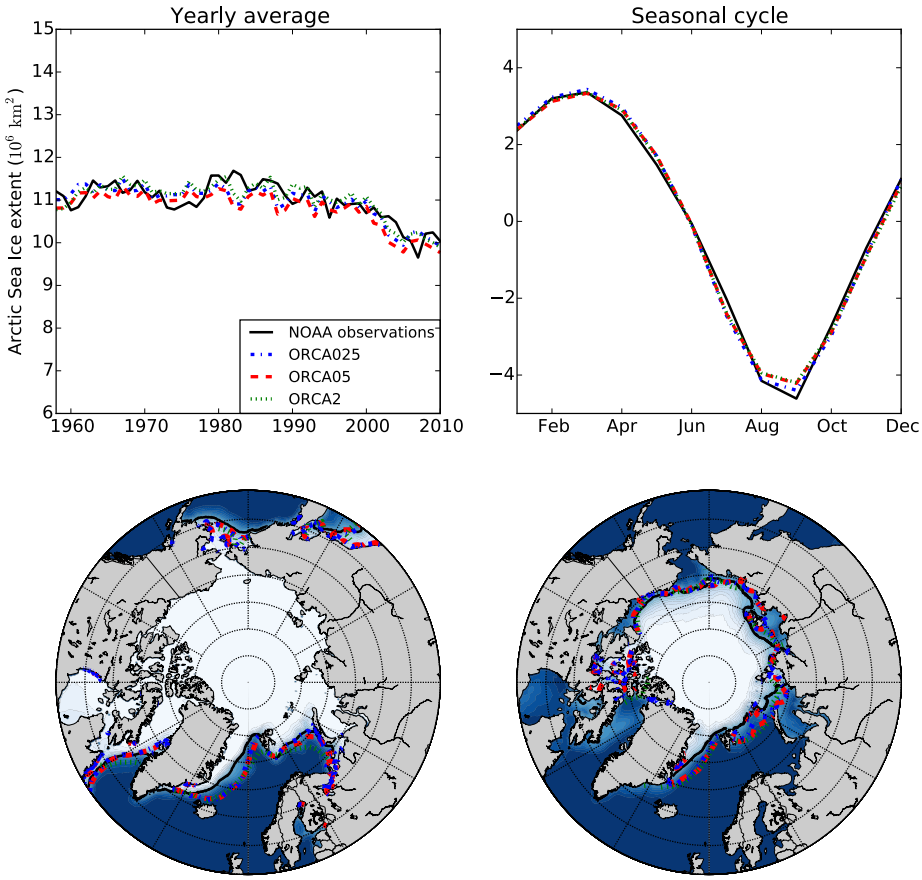

Figure 3. Sea-ice concentration in the Arctic from 1960 to 2012 comparing microwave-based observations from NOAA (black) to simulated results from ORCA2 (green), ORCA05 (red), and ORCA025 (blue). Shown are the yearly average (top left), and after detrending, the average (climatological) seasonal cycle over 1958–2010 (top right), average sea-ice extent in winter (December, January, February) (bottom left), and summer (bottom right). The lines on the maps show the 50% sea-ice cover for the three model resolutions and the observations. The white color indicates the observed sea-ice concentration.

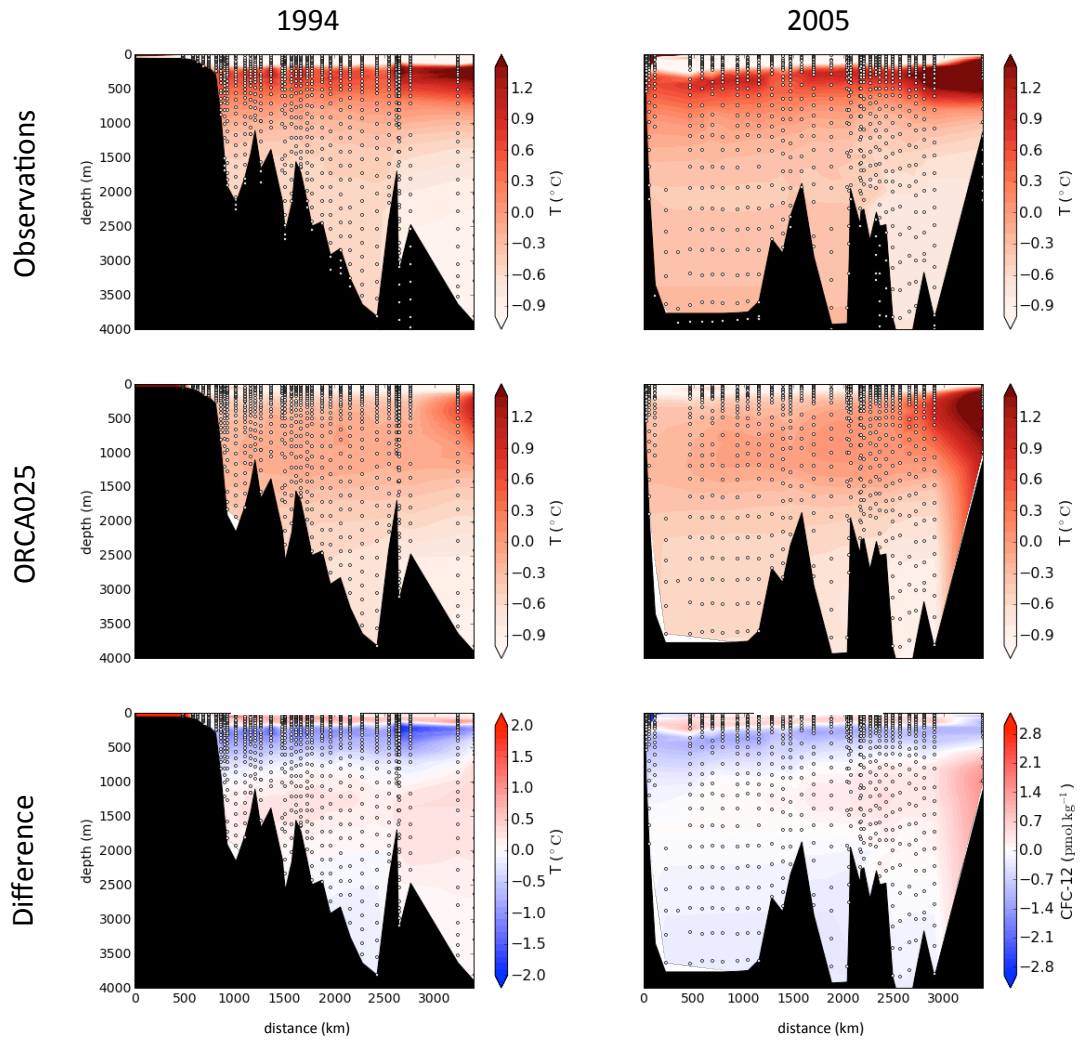

Figure 4. Temperature along the 1994 Arctic Ocean Section (AOS94) cruise (left) and the Beringia/HOTRAX 2005 expedition (right), both trans-Arctic transects (Fig. 1). The observations (top) are compared to simulated results from ORCA025 averaged over summer of the respective year (middle). The difference (model − observations) is shown at the bottom. The location of the sections is shown in Fig. 1.

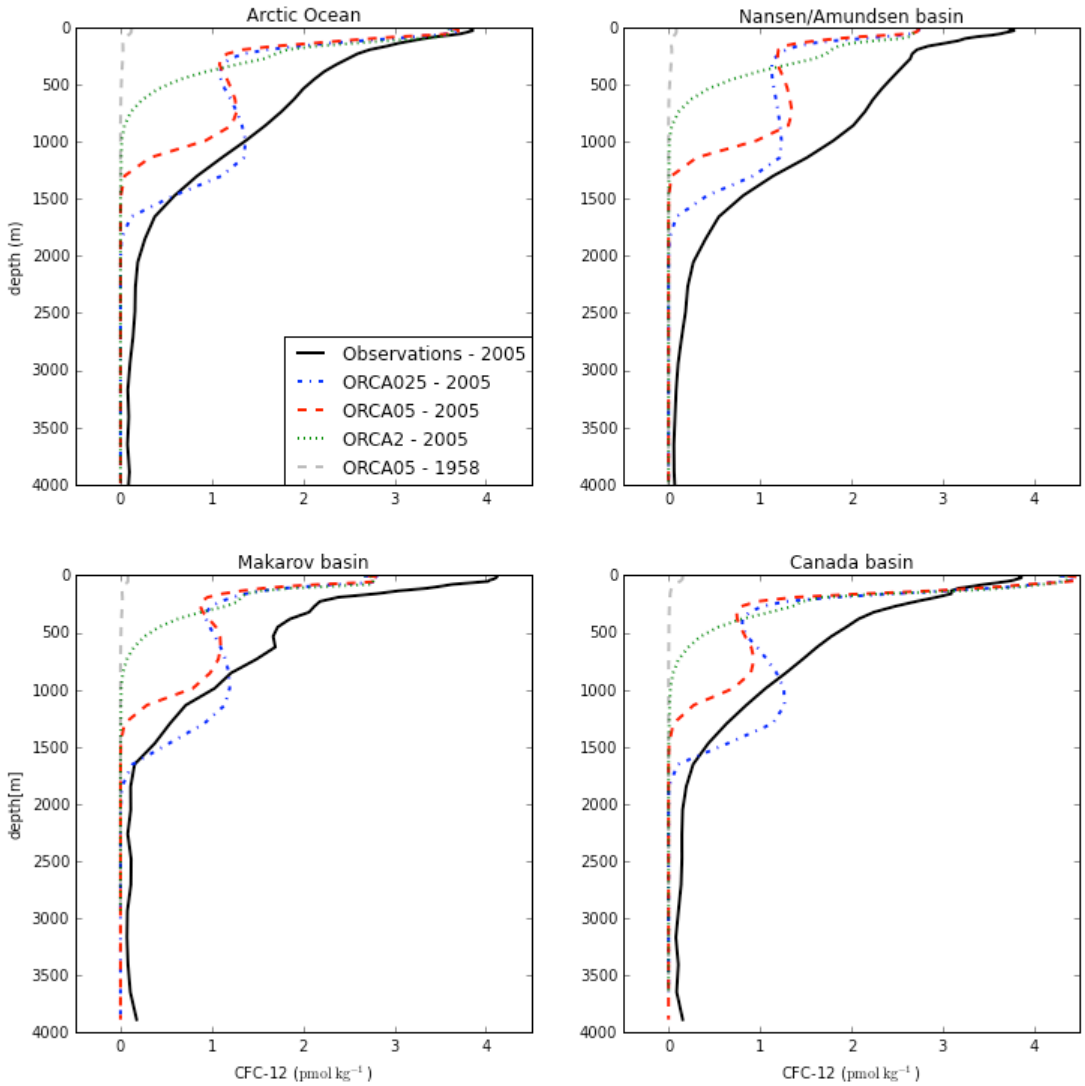

Figure 5. Profiles of CFC-12 for observations (black) and the ORCA025 (blue), ORCA05 (red), and ORCA2 (green) model along the 2005 sections. Shown are distance-weighted mean across each section (top left), the Nansen and Amundsen basins (top right), the Canada basin (bottom left), and the Makarov basin (bottom right).

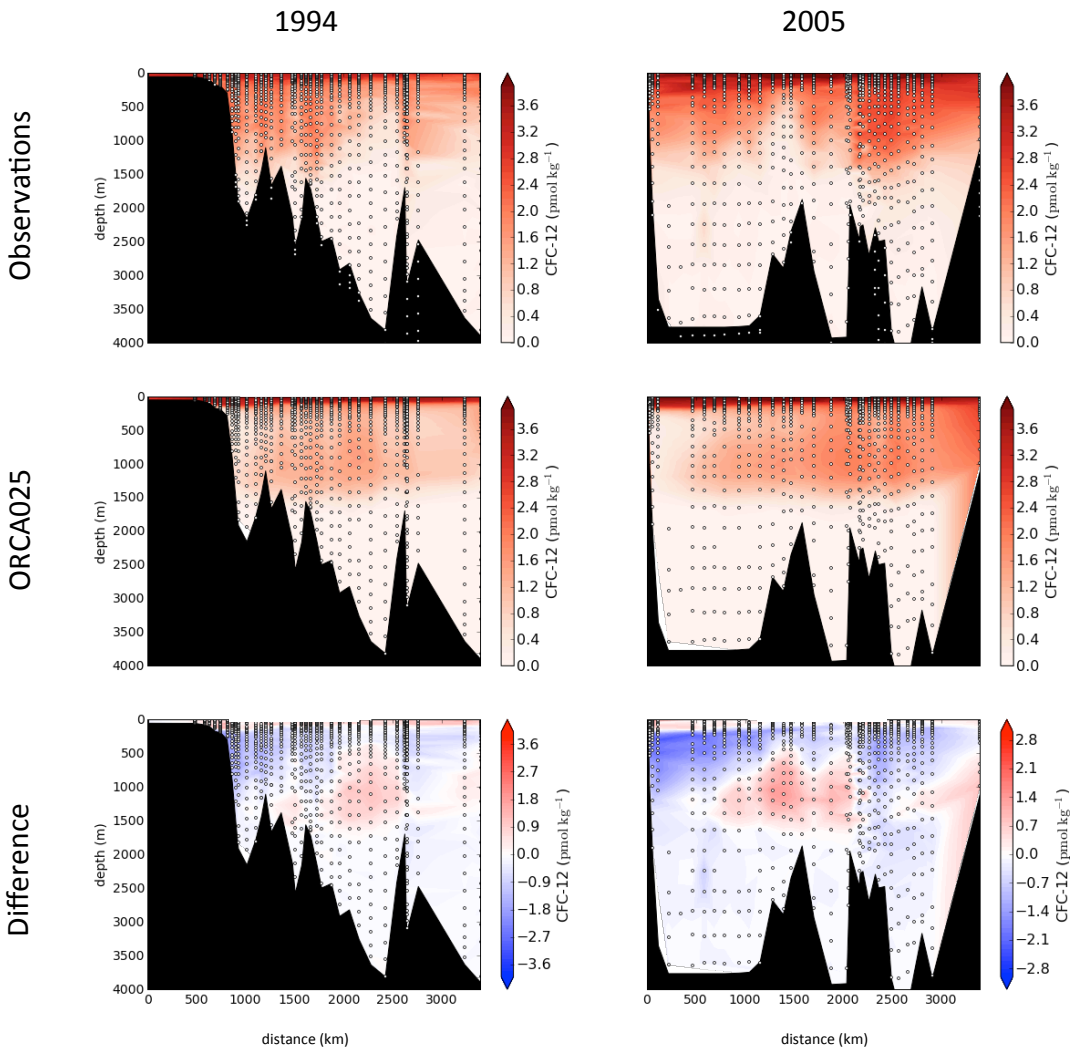

Figure 6. CFC-12 sections along the AOS94 section (left) and the Beringia section (right). The observations (top) are compared to the simulated summer means (middle) and model−data difference is shown at the bottom.

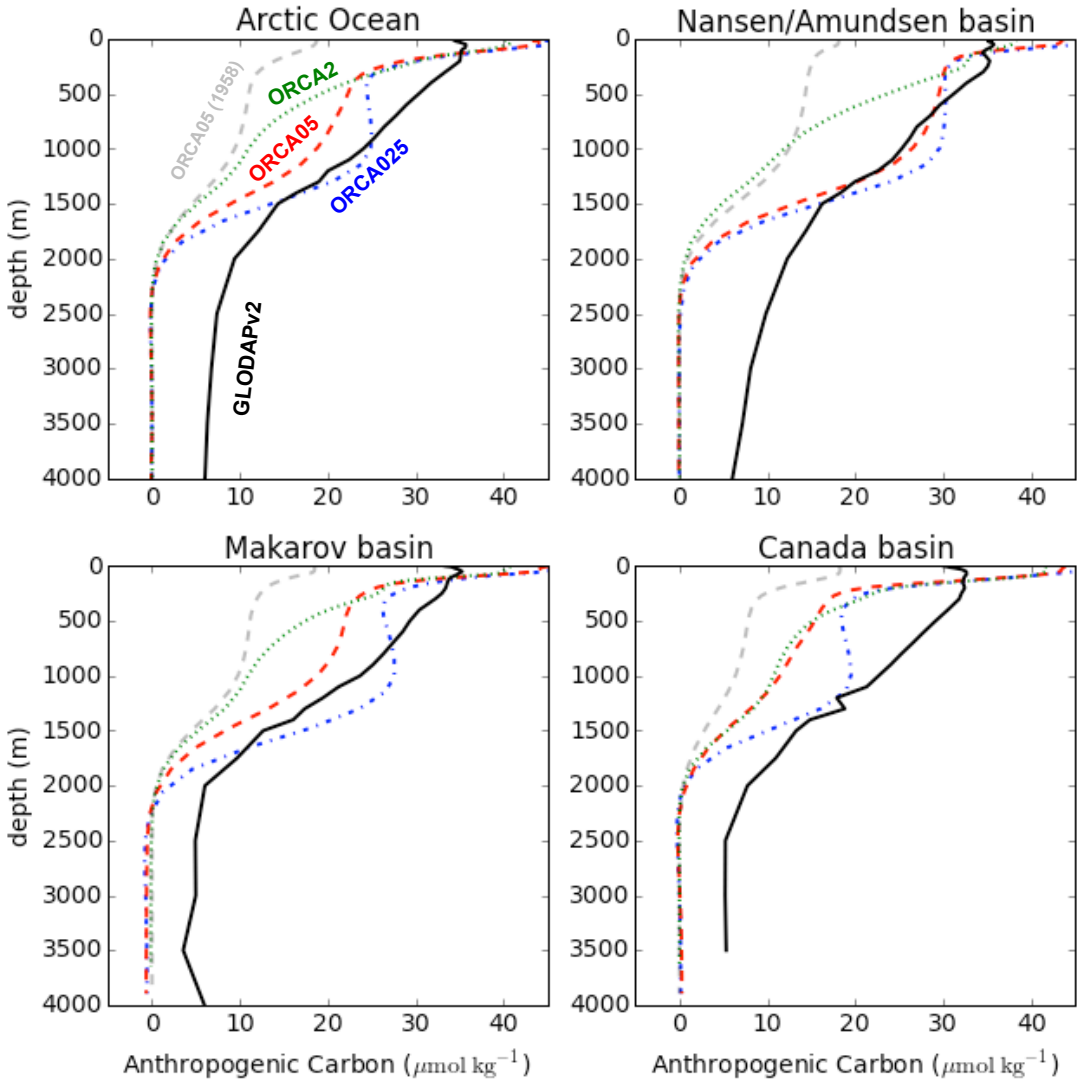

Figure 7. Area-weighted vertical profiles of ~~C_{ant}~~ C_{ant} concentrations for GLODAPv2 data-based estimates (black), ORCA2 (green), ORCA05 (red) and ORCA025 (blue) over the entire Arctic Ocean corrected for the starting year by the perturbation approach simulations. The vertical profile in 1958, when the simulation is divided for the three resolutions, is shown in light grey.

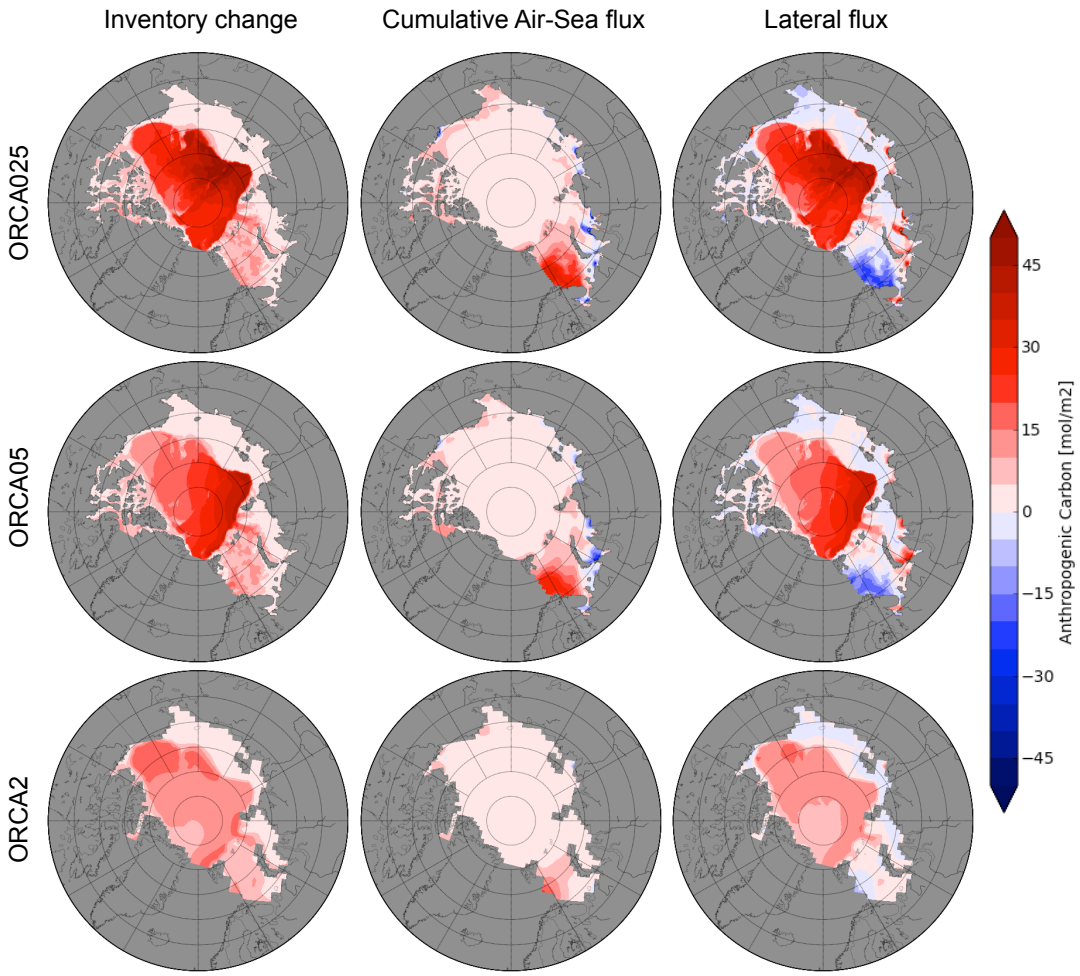

Figure 8. Inventory change (left), cumulative air-sea flux (middle), and the lateral flux calculated as the difference of inventory change and air-sea flux (right) of ~~C_{ant}~~ C_{ant} for the period from 1960 to 2012 for the ORCA025 (top), ORCA05 (center), and ORCA2 (bottom) model configurations.

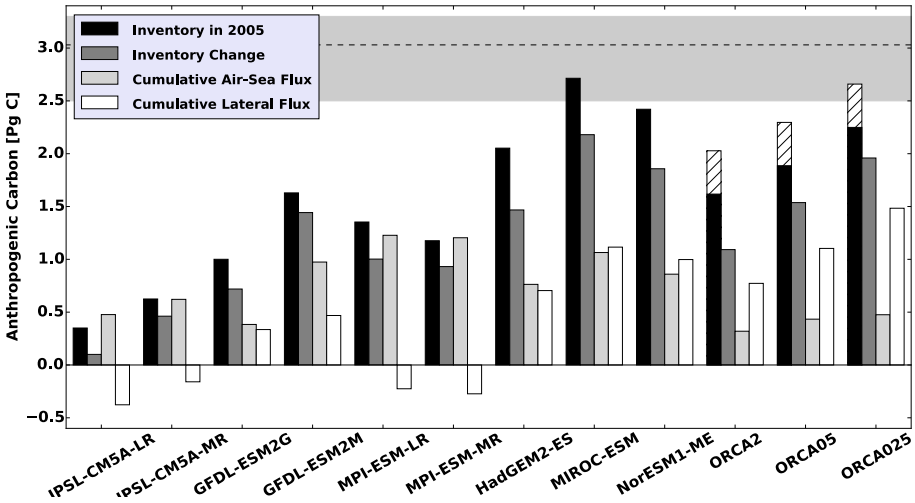

Figure 9. Comparison of results for the Arctic Ocean from the three resolutions of NEMO-PISCES and the nine Earth System Models that participated in CMIP5. Shown are the ~~C_{ant}~~ C_{ant} inventory in 2005 (black), the inventory change of ~~C_{ant}~~ C_{ant} (dark grey) between 1960 and 2012, the corresponding cumulative air-sea flux of ~~C_{ant}~~ C_{ant} (light grey) and the cumulative lateral flux of ~~C_{ant}~~ C_{ant} (white). Also indicated are the ~~corrected~~ estimate by Tanhua et al. (2009) (dashed black line) and the associated uncertainty estimates (grey background). The inventory correction of the biogeochemical simulations using the perturbation approach is added to the results of the biogeochemical simulations as striped bars.

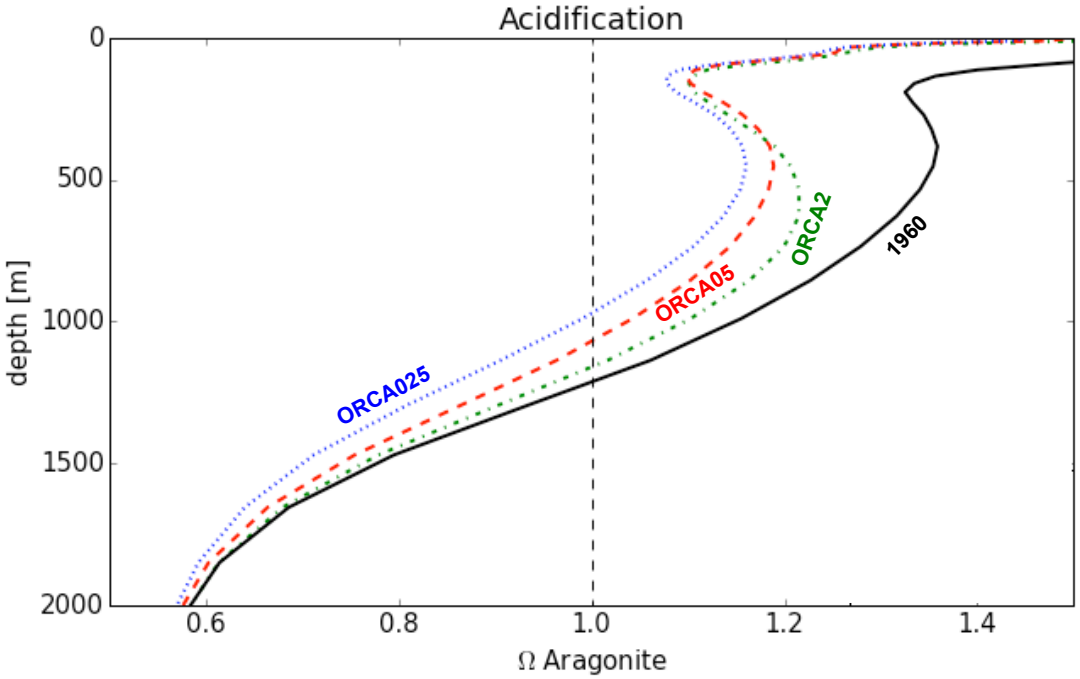

Figure 10. Profiles of Ω_A ~~after the early industrial period period simulated only in ORCA05 (1870–1957), after intializing the other models in 1958. Results are shown~~ for ORCA05 in 1960 (black solid) as well as ORCA2 (green dot-dash), ORCA05 (red dashes), and ORCA025 (blue dots) in 2012. The vertical black dashed line indicates the chemical threshold where $\Omega_A = 1$. Where that vertical line intersects the other curves indicates the depth of the ASH in each case.

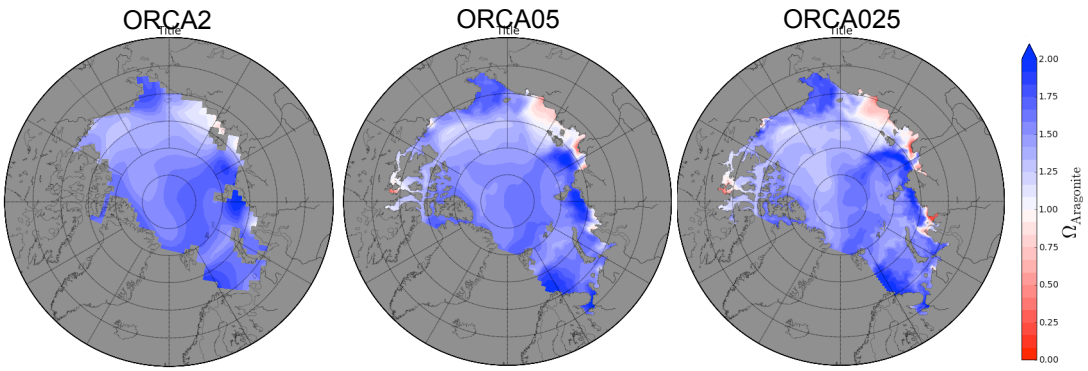

Figure 11. Surface Ω_A for ORCA2, ORCA05 and ORCA025 (from left to right) in August 2012.